

NEURAL MECHANISMS IN PROCESSING OF EMOTION IN REAL AND  
VIRTUAL FACES USING FUNCTIONAL-NEAR INFRARED SPECTROSCOPY  
(FNIRS)

by

Dylan Rapanan

A thesis submitted to the  
School of Graduate and Postdoctoral Studies  
in partial fulfillment of the requirements for the degree of

**Masters of Science in Computer Science**

Faculty of Science  
Ontario Tech University  
Oshawa, Ontario, Canada

© Dylan Rapanan 2025

## Abstract

As avatars permeate social media, gaming, and telecommunications, understanding how the brain reads emotions from virtual faces is increasingly important. We recorded functional near-infrared spectroscopy (fNIRS) data from adults viewing real photographs and matched computer-generated faces expressing Anger, Disgust, Fear, Joy, Sadness, Surprise, or Neutral (control). General-linear-model mapping revealed higher activation in virtual faces in the left occipital region, and higher activation in Neutral and Surprise compared to the other emotions in parietal and occipital regions. Functional-connectivity analysis revealed higher connectivity in real faces across the brain, and higher connectivity across the brain in Anger and Fear compared to the other emotions. Collectively, the results demonstrate differences in activation in occipital areas, and differential processing of face and emotion types across the whole brain. These neural signatures provide quantitative targets for refining the realism and emotional efficacy of digital characters in virtual and augmented environments.

## Acknowledgements

\*\* Put your Acknowledgements here. \*\*\*

# Contents

<b>Abstract</b>	ii
<b>Acknowledgment</b>	iii
<b>1 Introduction</b>	1
<b>2 Methodology</b>	2
2.1 Participants . . . . .	2
2.2 Stimuli and apparatus . . . . .	4
2.2.1 Stimuli . . . . .	4
2.2.2 Apparatus . . . . .	4
2.3 Design and procedure . . . . .	6
2.3.1 Design . . . . .	6
2.3.2 Procedure . . . . .	7
2.4 Analyses . . . . .	8
2.4.1 fNIRS preprocessing . . . . .	9
2.4.2 Activation magnitude with General Linear Model (GLM) . . . . .	10
Design Matrix . . . . .	11
Contrast Computation . . . . .	12
2.4.3 Network mapping with Functional Connectivity Analysis . . . . .	13
Paired Sample t-tests . . . . .	14

ROI Chord Plots . . . . .	14
2.4.4 Memory Task Analysis . . . . .	14
<b>3 Results</b>	<b>16</b>
3.1 Activation magnitude . . . . .	16
3.1.1 Face Type differentiated by left-occipital activity . . . . .	16
3.1.2 Emotion differences in parietal and occipital regions . . . . .	17
3.1.3 Face Type $\times$ Emotion differences in occipital regions . . . . .	20
3.2 Functional Connectivity . . . . .	21
3.2.1 Face Type differentiated by greater connectivity for real faces .	21
3.2.2 Emotion differentiated by higher connectivity for Anger and Fear	23
3.2.3 Face Type $\times$ Emotion differentiated by higher connectivity for real faces in Anger, Disgust, and Neutral . . . . .	26
3.3 Higher accuracy for real faces in the memory task . . . . .	28
<b>4 Discussion</b>	<b>30</b>
4.1 Limitations and Future Directions . . . . .	30
4.2 Conclusion . . . . .	30
<b>Bibliography</b>	<b>30</b>
<b>Appendix</b>	<b>35</b>
<b>A GLM Contrasts</b>	<b>36</b>
<b>B Functional Connectivity Contrasts</b>	<b>41</b>
<b>C Memory Task</b>	<b>48</b>
C.1 ANOVA Results . . . . .	48
C.2 Memory Task No Response Distribution . . . . .	49

# List of Tables

A.1	Table of contrast results from the GLM analysis.	36
B.1	Group level <i>t</i> -tests and Sum of Significantly different channels averaged across ROIs.	42
C.1	Two-way ANOVA results for the effect of Face Type and Emotion and their interaction on the correct responses.	48

# List of Figures

2.1	Participant signal quality and inclusion flow . . . . .	3
2.2	Montage depictions . . . . .	5
2.3	Brain region map for ROI grouping . . . . .	6
2.4	Experimental paradigm overview . . . . .	8
2.5	Preprocessing steps for fNIRS data . . . . .	9
2.6	Sample design matrix for GLM . . . . .	12
3.1	GLM: Real vs. Virtual Faces . . . . .	17
3.2	GLM: Emotion vs. Neutral . . . . .	18
3.3	GLM: Emotion vs. Surprise . . . . .	19
3.4	GLM: Neutral vs. Surprise . . . . .	20
3.5	GLM: Face Type $\times$ Emotion Contrasts . . . . .	21
3.6	FC: Real vs. Virtual . . . . .	22
3.7	FC: Emotion Contrasts (Fear and Anger) . . . . .	23
3.8	FC: Summary of Contrasts by Emotion Pair . . . . .	24
3.9	FC: Count of Significantly Different Channel Pairs by ROI . . . . .	25
3.10	FC: Face Type $\times$ Emotion Contrasts . . . . .	27
3.11	Correct Memory Task Responses by Face Type and Emotion . . . . .	29
B.1	FC: Additional emotion contrasts . . . . .	41
C.1	Memory Task No Response Distribution . . . . .	49

# **Chapter 1**

## **Introduction**

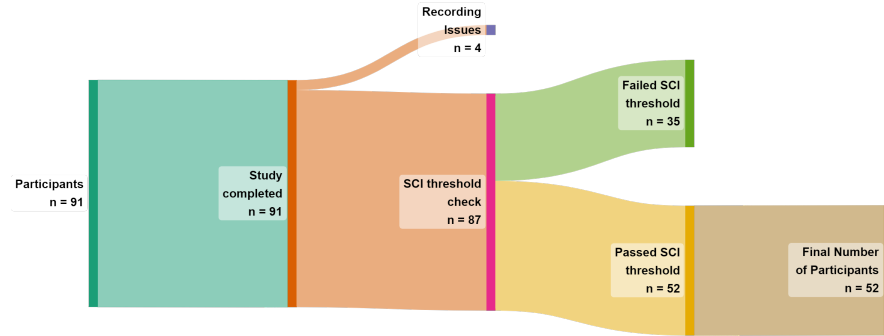
# Chapter 2

## Methodology

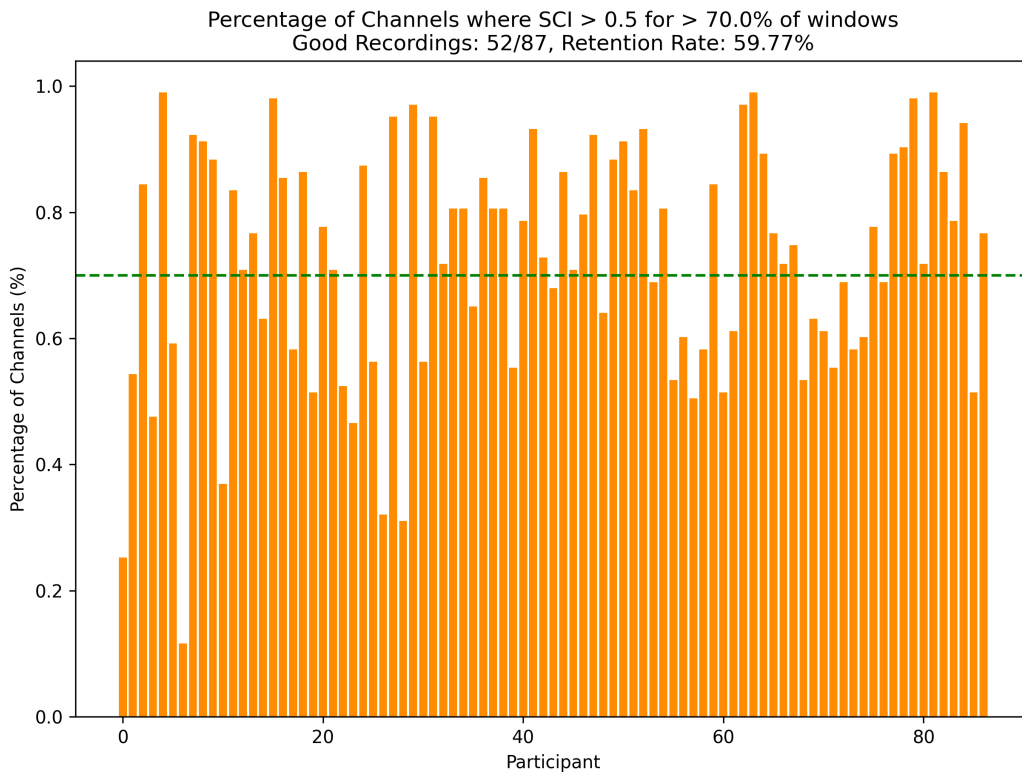
### 2.1 Participants

Ninety-one participants were recruited from Ontario Tech University's undergraduate student body through SONA. Participation flow is illustrated in Figure 2.1a. Four participants were removed due to equipment recording issues. Participants were then screened on inclusion criteria for a) task attention, and b) fNIRS signal quality. For attention, participants were required to achieve  $\geq 60\%$  accuracy on the behavioral memory task (chance accuracy = 50%) to ensure sufficient engagement. One participant failed to meet this criterion. The remaining 87 participants (69 females and 18 males,  $M = 21.09$ ,  $SD = 5.91$ , range = 17 to 51) were analyzed in the behavioral memory task. For neural analyses, signal quality of remaining 87 participants by computing the Peak Spectral Power (PSP) and the Scalp Coupling Index (SCI) (Pollonini et al., 2016). Measures were calculated using a 5-second sliding window across all channels (Bulgarelli et al., 2025; Hernandez and Pollonini, 2020). fNIRS inclusion criteria were: 1) PSP  $> 0.1$  and SCI  $> 0.5$  for more than 70% of the windows in a single channel, labelled "good signal quality" (Holmes et al., 2024), and 2)  $> 70\%$  of the channels for a single participant were marked as "good". Thirty-five participants failed to meet these criteria, illustrated in Figure 2.1b,

and were removed prior to data analysis. The final sample consisted of 52 participants (39 females and 13 males,  $M = 21.62$ ,  $SD = 6.67$ , range = 17 to 51). The study was approved by Ontario Tech's Research Ethics Board (REB: 17656).



(a) Sankey diagram showing the flow of participants through each stage of inclusion/exclusion in the study.



(b) Percentage of Channels where SCI > 0.5 for > 70% of the windows. The green dashed line represents the threshold of 70% of windows that each participant must meet to be included in the analysis.

Figure 2.1: (A) Participant inclusion flow diagram. (B) SCI signal quality inclusion threshold.

## 2.2 Stimuli and apparatus

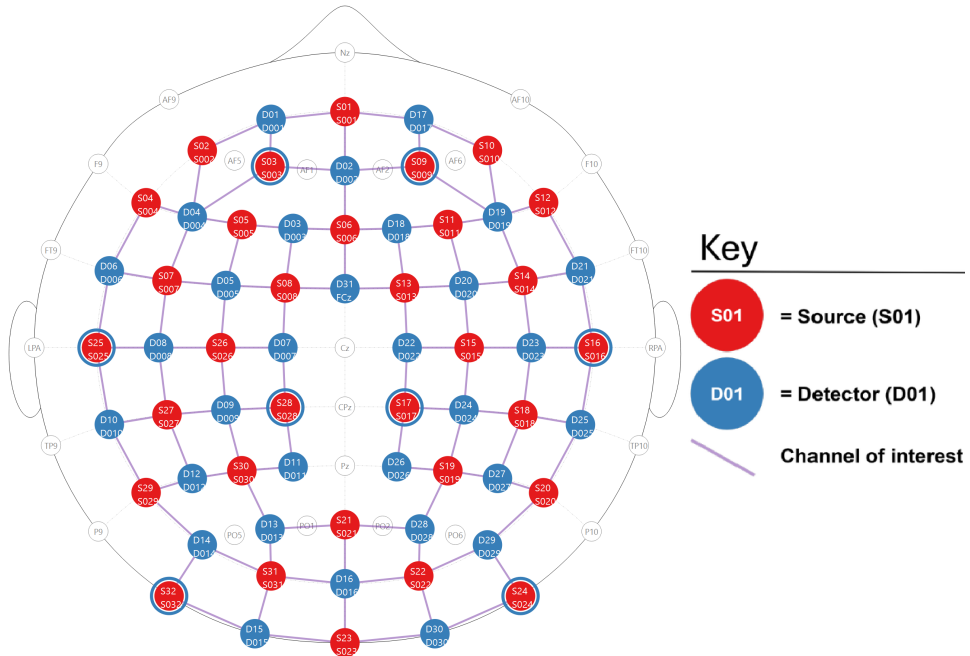
### 2.2.1 Stimuli

One hundred and forty images of facial expressions from the RADIATE and UIBVFED datasets were used ([Conley et al., 2018](#); [Oliver and Amengual Alcover, 2020](#)). Then adult models (5 males and 5 females) from each dataset were identified and matched between-sets on face shape, sex, skin tone, and hair colour. Images of each model expressing seven emotions (anger, disgust, fear, happiness, sadness, surprise, neutral) were selected. Expressions were selected for each model, that closely align with Ekman's 6 basic emotions + neutral ([Ekman, 1992](#)). UIBVFED images were cropped to the same size as RADIATE images.

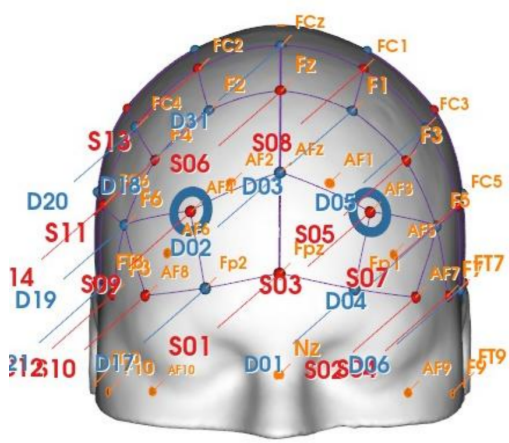
### 2.2.2 Apparatus

Participants were tested individually in a quiet dedicated testing room. Stimuli were presented on a Dell U2415 24-inch monitor at 1920x1200 60Hz. Participants were seated in a comfortable non-movable chair, with the monitor placed at eye level. Stimuli were presented using PsychoPy3 Experiment Builder (v2024.1.5) ([Peirce et al., 2019](#)). Participant brain activity was recorded using Aurora fNIRS while participants completed the task. fNIRS data was collected using two NIRSport2 systems (NIRx Medical Technologies, Berlin, Germany). Each NIRSport2 system was equipped with 16 source and 16 detector optodes, and daisy-chained together for a high density 32x32 optode configuration. Each neighboring pair of source and detector optode is referred to as a channel, resulting in a total of 103 HbO + 103 HbR channels (plus 16 short distance channels). The average distance between source and detector optodes was 30 mm, and 7mm for short distance channels, which were placed on a flexible fNIRS head cap (NIRScap) 58 cm in circumference. The optodes were arranged in a high density 32x32 montage with one bundle of short distance channels, as shown in Figure 2.2. This montage was designed to cover

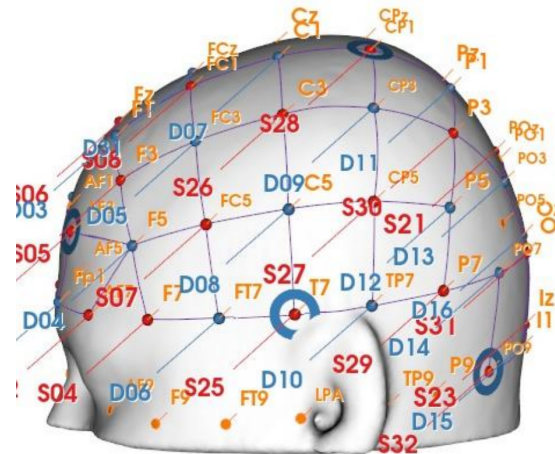
a maximally large area of the brain, given increasing evidence that emotion processing is not localized to specific discrete areas of the brain, rather distributed across the brain (Lindquist et al., 2012). The fNIRS cap and optodes were positioned following the 10-20 international coordinate system. Light was emitted at 760 nm and 850 nm wavelengths, and the sampling rate was approximately 6.105 Hz.



(a) 2D depiction of the montage.



(b) 3D front view of the montage.



(c) 3D side view of the montage.

Figure 2.2: Depictions of the high density 32x32 optode montage. Red circles represent sources, blue circles represent detectors, purple lines represent channels, and blue rings around sources represent the locations of the 8 short distance detectors.

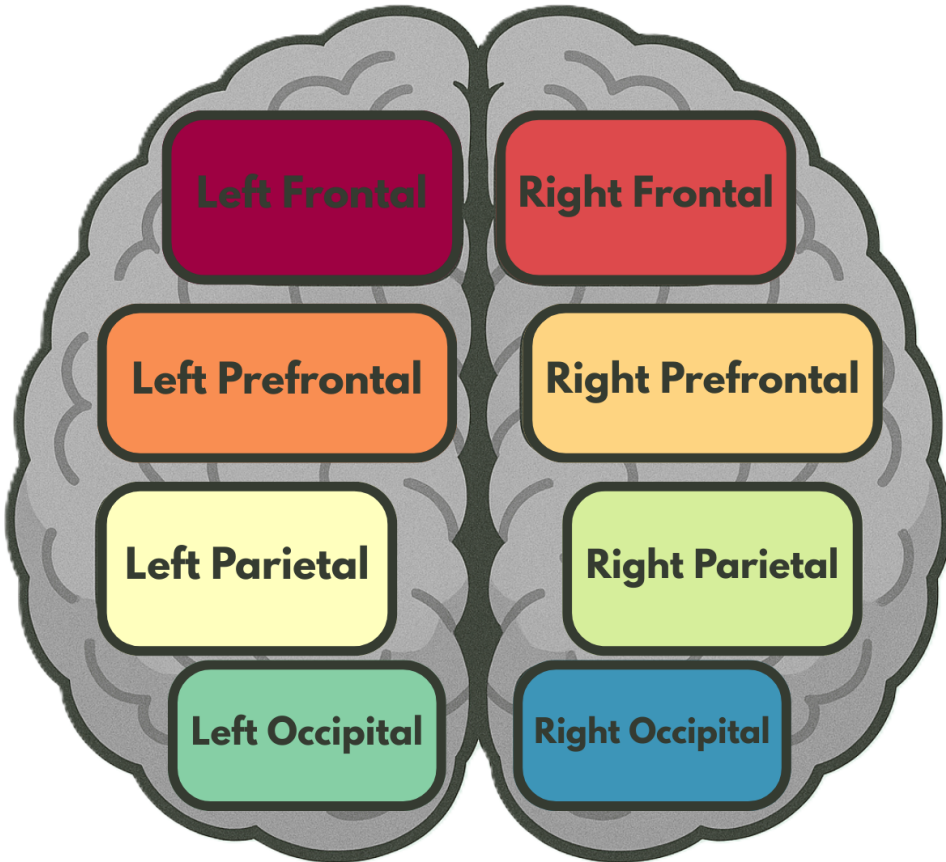


Figure 2.3: Brain region map, showing the regions of interest (ROI's) that the channels were grouped into for certain analyses.

## 2.3 Design and procedure

### 2.3.1 Design

A full-factorial Face-type (2 levels: Real, Virtual)  $\times$  Emotion (7 levels: Anger, Disgust, Fear, Joy, Sadness, Surprise, Neutral)  $\times$  Model (4)  $\times$  Sex (2 levels: Male, Female)  $\times$  Repetition (4) experimental design was used, with each participant presented with 448 images. Stimuli were blocked and counterbalanced by Face-type and Emotion. Within each of the 56 Face-type-Emotion Blocks, participants were presented with 8 distinct model faces (4 male, 4 female).

### 2.3.2 Procedure

Following consent and briefing, participant head size was measured and a size-appropriate fNIRS cap fitted. A signal optimization routine was then run within Aurora fNIRS to optimize participant channel signal levels. This routine worked by increasing source brightness in a stepwise manner, until the optimal signal levels for all channels was reached. Following optimization, participants were told that they would be presented with a series of facial expression images and asked to identify whether a probe face matched one of the faces they saw in the preceding block. Room lights were then switched off to avoid interference with the fNIRS cap, and participants were monitored from an adjacent room with a live camera feed.

The experiment began with instructions presented on screen. The trial timeline, shown in Figure 2.4, consisted of three main epochs: fixation cross, block presentation, and participant feedback. Each Block began with a fixed cross presented for 16 seconds, followed by 8 facial images. Facial images were each presented for 1.5 seconds, with a 250-750 ms ( $M=500$  ms) interstimulus interval (ISI) between each face. To maintain participant attention, participants completed a memory task after each block. In the task, participants were presented with a model image with the same emotional expression as the rest of the block's images, and asked if the model was shown in the preceding block of 8 faces, with feedback provided using the keyboard (y/n). The probe face has a 50% chance of either being in the previous block or not. The experiment continued after seven seconds if no feedback was provided. Most participants only failed to respond to 1-2 blocks of the 56 blocks, with only a handful of participants failing to respond to up to 5 blocks, as illustrated in Figure C.1. Participants were given a break every seven blocks, and prompted to enter the space bar when they are ready to continue the experiment. After the experiment was completed, the experimenter(s) entered the room, removed the fNIRS cap, and the participant was debriefed about the experiment. Participation in the experiment took approximately 35 minutes.

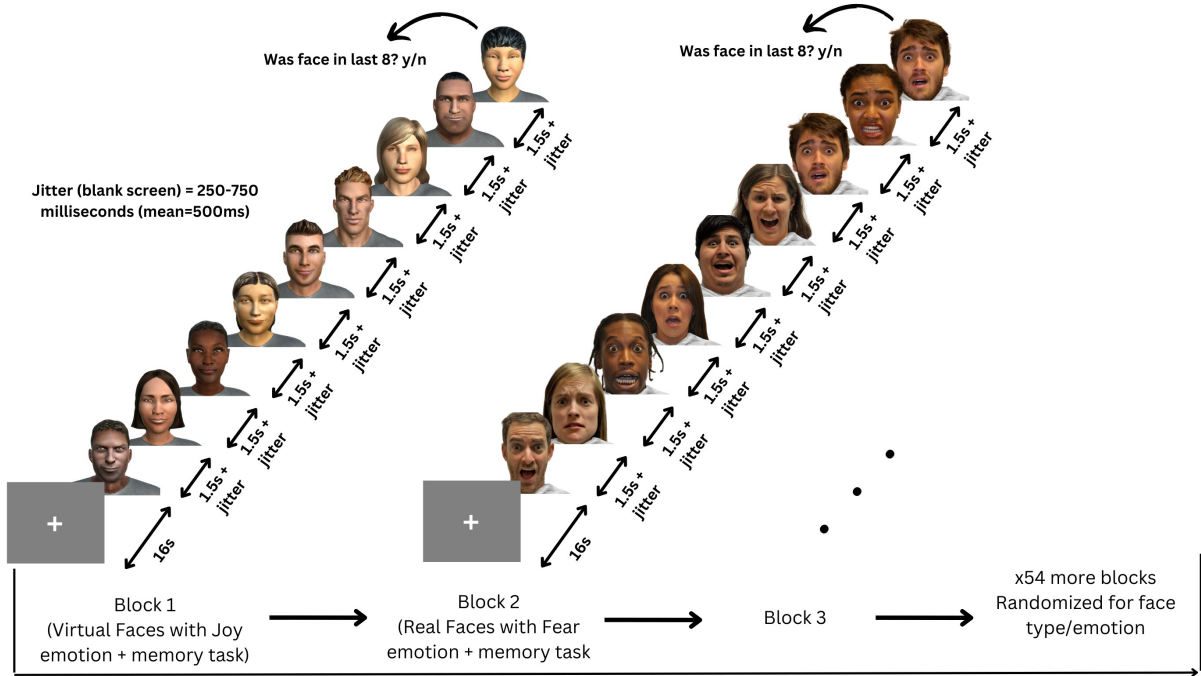


Figure 2.4: Participants viewed 56 blocks of 8 faces, each block being either all real or all virtual faces. Every face in a block displayed the same emotional expression, one of: anger, disgust, fear, happiness, sadness, surprise, neutral.

## 2.4 Analyses

All fNIRS data was preprocessed and analyzed with Python 3.11.9 using MNE (version 1.9.0) ([Gramfort et al., 2013](#)) and MNE-NIRS (version 0.7.1) ([Luke et al., 2021](#)), which used the Nilearn package (version 0.9.2). Data were analyzed with a General Linear Model (GLM), followed by a functional connectivity analysis. The memory task was analyzed in Python using the statsmodels package (version 0.14.4) ([Seabold and Perktold, 2010](#)).

### 2.4.1 fNIRS preprocessing

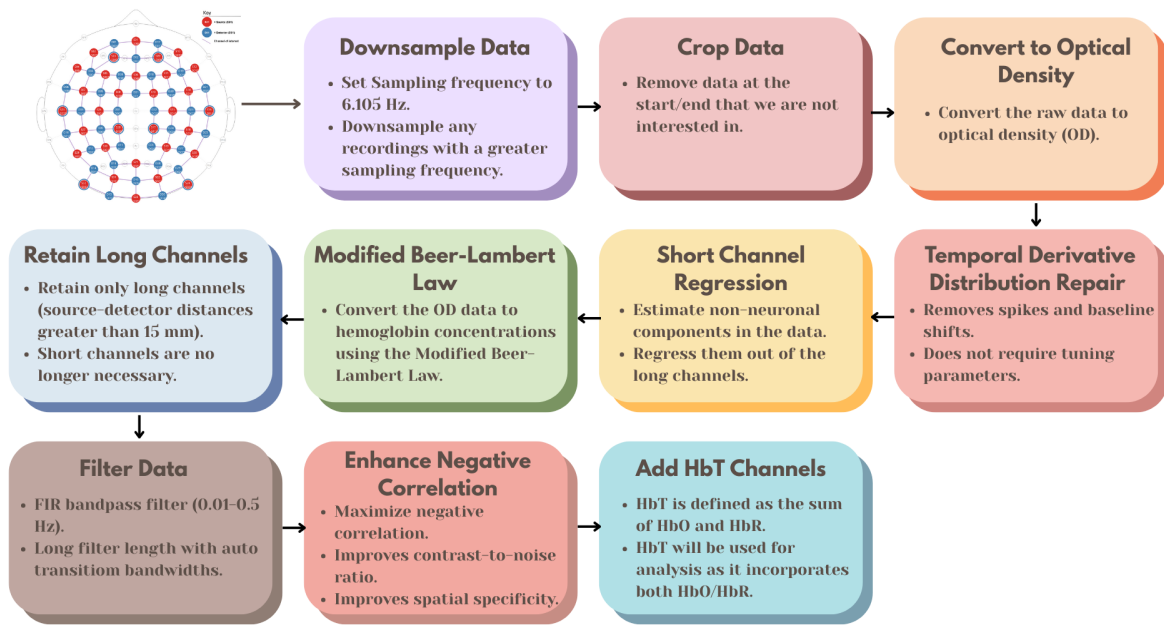


Figure 2.5: Preprocessing steps for fNIRS data, from the raw data to the fully processed data.

The preprocessing steps for the fNIRS data, as shown in Figure 2.5, were as follows:

- 1) Downsample the data if the sampling frequency is greater than 6.105 Hz, the initial two datasets were sampled higher than 6.105 Hz, and the sampling frequency should be consistent across all datasets.
- 2) Crop the data to the first and last annotation. This gets rid of the extra data at the beginning and end of the recording that are not of interest.
- 3) Convert the raw data to optical density.
- 4) Apply temporal derivative distribution repair to the OD data (Fishburn et al., 2019). TDDR is effective at removing spikes and baseline shifts from the data.
- 5) Apply short channel regression to the OD data (Scholkmann et al., 2014). Short channels are used to estimate the superficial hemodynamics (non-evoked/extracerebral/systemic components) in the data, and then regress it out of the long channels (Tachtsidis and Scholkmann, 2016).
- 6) Convert the OD data to hemoglobin concentrations using the modified Beer-Lambert law. The MBLL relates the change in light attenuation to the change in hemoglobin concentration of chromophores in the

tissue (Kocsis et al., 2006). 7) Retain only long channels (source-detector distance > 15 mm). Since the short channels have already been regressed out, it is no longer necessary to keep them in the data. 8) This FIR bandpass filter extracts signal components in the 0.01-0.5 Hz range, it uses a long filter length (2015 samples) with automatically determined transition bandwidths by MNE-Python (Pinti et al., 2019). 9) Maximizes negative correlation between HbO and HbR (Cui et al., 2010). This method removes spikes, improves contrast-to-noise ratio, and improves spatial specificity of the data. 10) Add HbT (hemoglobin total) channels to the data. HbT is defined as the sum of HbO and HbR. Often, fNIRS studies will only use either one of HbO or HbR channels (more frequently HbO), leaving out one channel with no justification (Kinder et al., 2022). Therefore, HbT channels are chosen, as HbT makes use of both HbO and HbR channels, and using both hemoglobin species improves the inferences as to where activation occurs (Hocke et al. (2018)).

Variable length epochs were created for each block of 8 faces, which were 14-18 seconds long (mean = 16s), depending on the ISI's (see 2.3.2). Epochs were sorted by Face Type (Real, Virtual), and Emotion (Anger, Disgust, Fear, Happiness, Sadness, Surprise, Neutral), and their interaction. Baseline correction was applied to remove any constant or slowly varying offsets in the data. The data was annotated with the onsets and offsets of each block, along with the duration and condition of each block. Block data were then analysed using a GLM and Functional Connectivity analysis.

#### 2.4.2 Activation magnitude with General Linear Model (GLM)

The General Linear Model (GLM) posits that the observed haemodynamic signal at each channel or Region of Interest (ROI) is a linear combination of task-related regressors convolved with a Hemodynamic Response Function (HRF), plus nuisance regressors (e.g., drift) and residual noise. Mathematically,

$$Y = X\beta + \epsilon, \quad (2.1)$$

where  $Y$  is the observed time series,  $X$  is the design matrix,  $\beta$  represents the parameters to estimate, and  $\epsilon$  denotes the residuals assumed to be Gaussian noise. Estimation is performed via ordinary least squares (OLS), yielding parameter estimates that quantify condition-specific activation amplitudes.

## Design Matrix

For each of the epochs, events are defined by their trial type (e.g., emotion or face type), and onsets/offsets relative to the procedure start, and duration. The design matrix is constructed using Nilearn's `make_first_level_design_matrix` by convolving a boxcar function (based on the event timing) with a canonical HRF, which is a model of the expected haemodynamic response to neural activity. The canonical HRF Statistical Parametric Mapping (SPM) ([Friston, 2007](#)) is chosen to model neurovascular coupling, this model captures the stereotypical rise and fall of the BOLD/fNIRS response. The cosine drift model was utilized, which incorporates discrete cosine transform (DCT) basis functions into the design matrix to model and remove low-frequency drifts. The selection of the high pass cutoff frequency is guided by the structure of the experimental design. The cutoff period is set to twice the duration of the longest inter-trial interval, and each fixation period between epochs (or blocks) is 16 seconds. Therefore, a cutoff period of 32 seconds (i.e., `high_pass=0.03125 Hz`) would be appropriate. This ensures that the drift model does not remove task-related signal components that occur at frequencies higher than the cutoff ([Luke et al., 2021](#)). The design matrix  $X$  and preprocessed time series are fed into MNE's `run_glm` function, which computes OLS estimates of  $\beta$  for each channel.

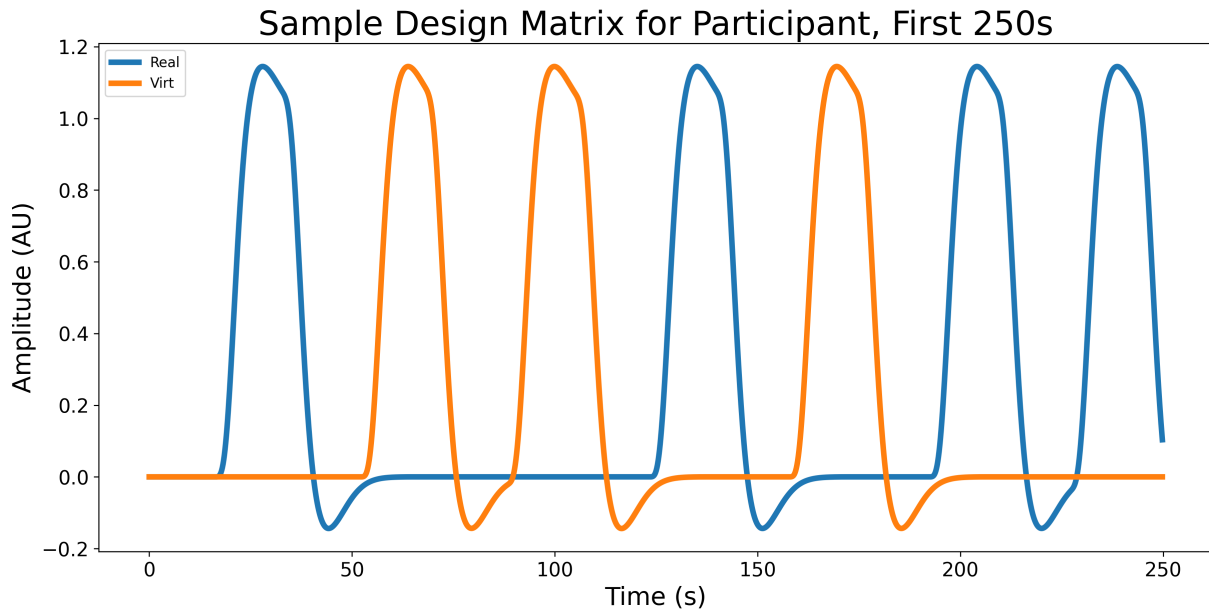


Figure 2.6: Sample design matrix for a single participant for the effect Face type, showing the first 7 blocks (250 seconds) of a single experiment. The design matrix is organized by condition (Blue for real, orange for virtual), this is the result of convolving the boxcar function with the canonical HRF SPM.

A two-way repeated measures GLM was conducted on participant's HbT responses by Face-type (2 levels: Real, Virtual) and Emotion (7 levels: Anger, Disgust, Fear, Joy, Sadness, Surprise, Neutral). Pairwise contrasts were then computed between conditions to identify effects of interest.

### Contrast Computation

All pairwise contrasts were generated between conditions by constructing an identity contrast matrix over design columns. For each pair of conditions ( $A, B$ ), the contrast vector is defined as:  $c = e_A - e_B$ , where  $e_A$  and  $e_B$  are the respective design matrix columns for conditions  $A$  and  $B$ . Contrasts are computed using MNE's `compute_contrast` function, which produces effect estimates and test statistics aggregated across channels. Since numerous statistical tests are performed across channels and contrasts,  $p$ -values were corrected for false discovery rate (FDR) using the Benjamini-Hochberg procedure (Singh and Dan, 2006) with a family-wise error rate of  $\alpha=0.05$ .

### 2.4.3 Network mapping with Functional Connectivity Analysis

To characterize the temporal coordination between fNIRS channels during face and emotion processing, functional connectivity matrices were computed using a continuous wavelet transform (CWT)-based spectral connectivity approach. CWT decomposes signals into simultaneous time-frequency representations, providing an optimal framework for fNIRS connectivity analysis by accommodating the non-stationary, physiological nature of hemodynamic signals. The morlet wavelet, a gaussian function modulated by a sine wave, was picked as they are suited to capture both slow neural rhythms and faster systemic fluctuations in fNIRS data ([Reddy et al., 2021](#)). Wavelet-based approaches have been widely adopted in the fNIRS literature for connectivity and even artifact correction ([Bergmann et al., 2023](#); [Hakim et al., 2023](#)) Coherence combines both phase and amplitude information into a single, normalized index, 0 (no coupling) to 1 (perfect coupling), and is a richer description of coupling than phase-only or amplitude-only metrics ([Bastos and Schoffelen, 2016](#)). For each participant, MNE’s `spectral_connectivity_time` function was applied to compute time-resolved coherence across pairs of channels, the average of this was taken across epochs to obtain a single channel-by-channel connectivity matrix for each condition. Each participants’ connectivity matrix was then averaged across participants to obtain a group-level connectivity matrix for each condition. fNIRS hemodynamics predominantly fluctuate in very low frequencies (0.01-0.5 Hz) ([Reddy et al., 2021](#)). The frequency range was narrowed to five evenly spaced frequencies between 0.2-0.5 Hz due to short epoch length, this range still targets systemic and neurogenic oscillations while avoiding high-frequency noise ([Xu et al., 2017](#)). Averaging across these closely spaced frequencies reduces data dimensionality, simplifying downstream statistical analyses without sacrificing sensitivity to coupling dynamics.

### Paired Sample t-tests

For each mode (Face type/Emotion), and pair of conditions (e.g., Joy vs. Fear), individual-level connectivity matrices were extracted, averaging across epochs and time points to obtain, per participant, a symmetric channel-by-channel coherence matrix. Because coherence values are bounded between 0 and 1 and exhibit skewed distributions ([Miranda de Sá et al., 2009](#)), Fisher's r-to-z transform (`atanh`) was applied to each matrix element to normalize the data prior to parametric testing. Paired t-tests for each unique channel pair ( $i > j$ ) were then conducted across participants using SciPy's `ttest_rel`. This directly tests whether mean connectivity differs between conditions, leveraging the paired design to increase statistical sensitivity ([Hu et al., 2023](#)). Given the large number of channel-pair tests, and similar to the GLM analysis above in [2.4.2](#),  $p$ -values were corrected for FDR using the Benjamini-Hochberg procedure ([Singh and Dan, 2006](#)) with a family-wise error rate of  $\alpha=0.05$ .

### ROI Chord Plots

To distill high-dimensional channel-by-channel connectivity into interpretable inter-regional summaries, we mapped individual fNIRS channels onto anatomically defined ROI's. This includes left and right frontal, prefrontal, parietal, occipital regions of the brain as shown in Figure [2.3](#), and the channels were grouped into these regions based on their location in the montage. Since multiple channels may map to the same pair of regions (e.g., several left prefrontal channels connecting to several right occipital channels), we aggregated all significant connections ( $p < 0.05$ ) between two regions by taking the mean of their t-values.

#### 2.4.4 Memory Task Analysis

Raw behavioral data captured from PsychoPy were preprocessed to identify participant keyboard responses. The total correct trials per participant were summed. Since each

block of faces was either all real or all virtual, and all had the same emotional expression (as discussed in 2.3.2), each y/n response was labeled with Face type and Emotion. An OLS model was fit with accuracy (converted to numeric 0/1) as the dependent variable and categorical predictors for Face Type, Emotion, and their interaction. The goal is to determine the main effects of these two factors individually, as well as their interaction, on response accuracy. A two-way Type III ANOVA (via `sm.stats.anova_lm(model, typ=3)`) provided  $F$ -statistics and  $p$ -values for main effects and interaction. This version of the ANOVA is especially suitable when interactions are included in the model, as it calculates each effect after accounting for all other terms.

# Chapter 3

## Results

### 3.1 Activation magnitude

#### 3.1.1 Face Type differentiated by left-occipital activity

A main effect of Face type was reported, with pairwise contrasts revealing greater activation for virtual faces compared to real faces, as shown in Figure 3.1.

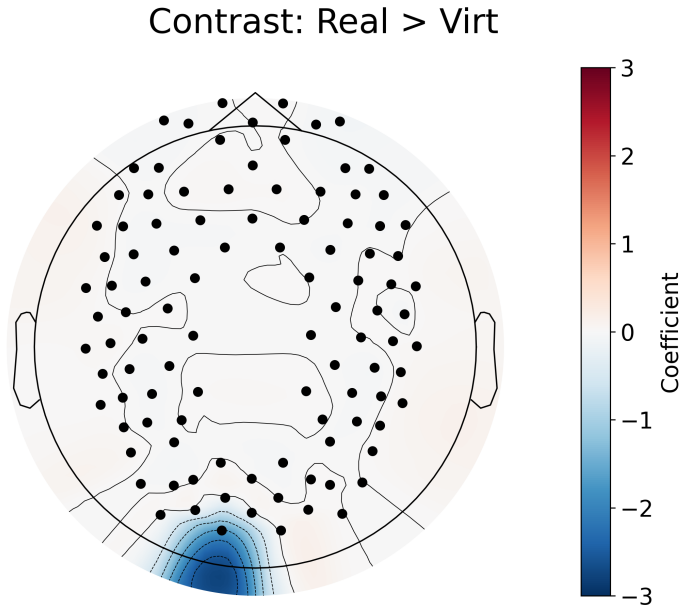


Figure 3.1: GLM contrast between real and virtual conditions which shows the differences in activation between the two conditions. Red signifies that condition 1 (real faces) has more activation in that area than condition 2 (virtual faces), while blue signifies that condition 2 (virtual faces) has more activation than condition 1 (real faces). The color bar on the right shows the coefficient of the contrast, which indicates the strength of the difference in activation between the two conditions.

### 3.1.2 Emotion differences in parietal and occipital regions

Pairwise contrasts with Neutral (control) and other emotions revealed significant differences in activation across several brain regions, as shown in Figure 3.2. Anger, Fear, and Joy elicited decreased activation in the right occipital region than Neutral. Joy was further associated with increased activation in the right parietal region, while Sadness showed reduced activation in the left frontal region relative to Neutral. These results indicate distinct neural activation patterns for each emotion when contrasted with the Neutral baseline, often involving the occipital region.

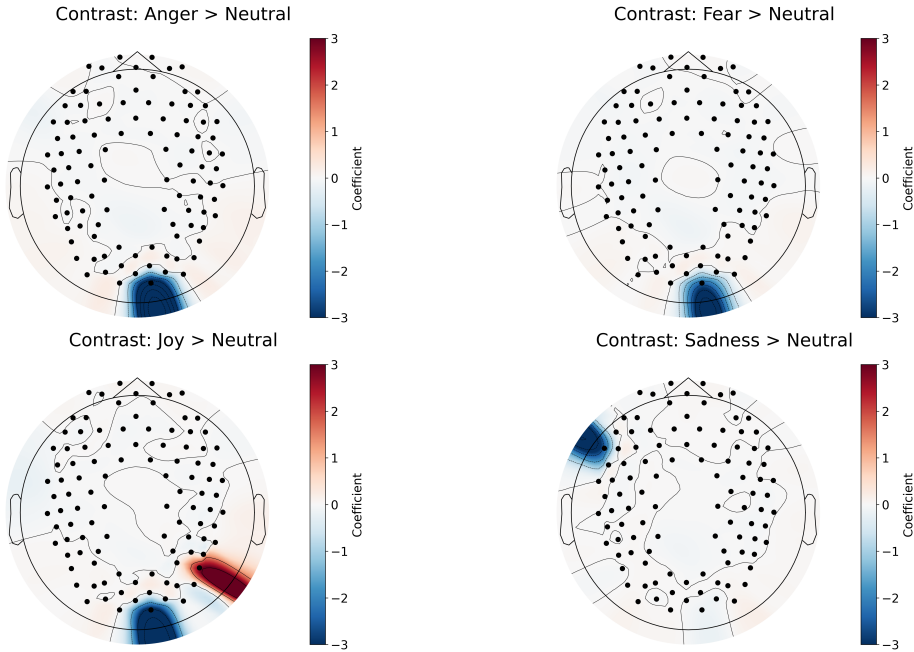


Figure 3.2: GLM results for the contrast between different emotions and neutral condition.

Exploratory contrasts further examined differences between Surprise and other emotions, as shown in Figure 3.3. Significant differences in activation were observed across multiple brain regions. Disgust and Joy showed decreased activation in the left prefrontal and right occipital regions relative to Surprise. Fear was associated with reduced activation in the right parietal region, while Sadness showed decreased activation in both the left frontal and right parietal regions. These findings suggest that Surprise was processed differentially than Neutral relative to other emotions, with differences in the prefrontal and parietal regions.

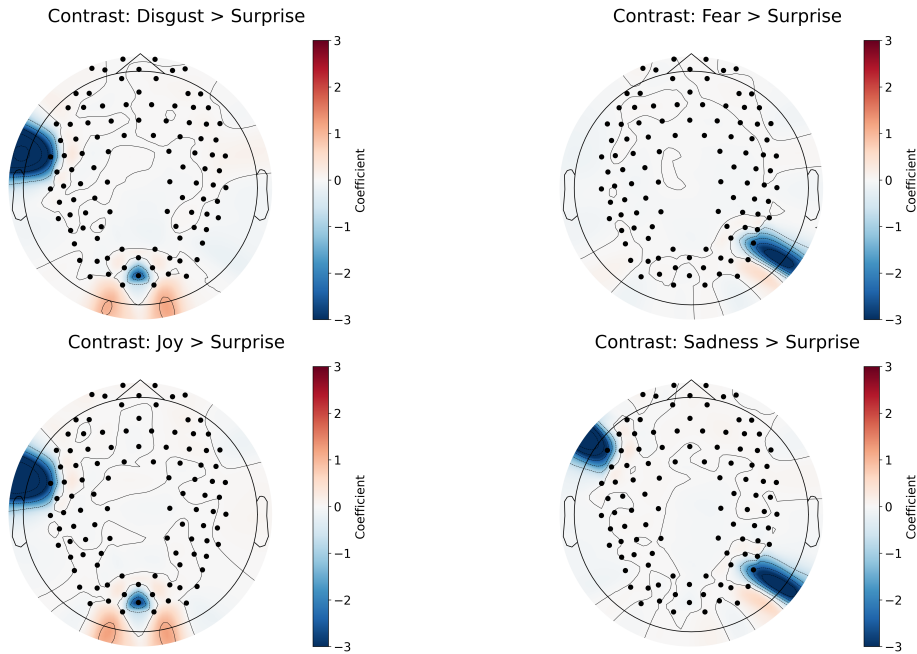


Figure 3.3: GLM results for the contrast between different emotions and surprise condition.

All combinations of emotion contrasts were performed, significant differences were only found between Neutral and the other emotions, and between Surprise and the other emotions. The Neutral > Surprise contrast revealed significant differences in the right parietal and right occipital regions, as shown in Figure 3.4. The right parietal region showed decreased activation (more activation for Surprise) while the right occipital region showed increased activation (more activation for neutral). Both Neutral and Surprise conditions elicit greater activation when compared to the other emotions, but when compared to each other, one emotion is not more activated than the other. This indicates that the neural response to Neutral and Surprise conditions is distinct, with each condition eliciting different activation patterns in specific brain regions.

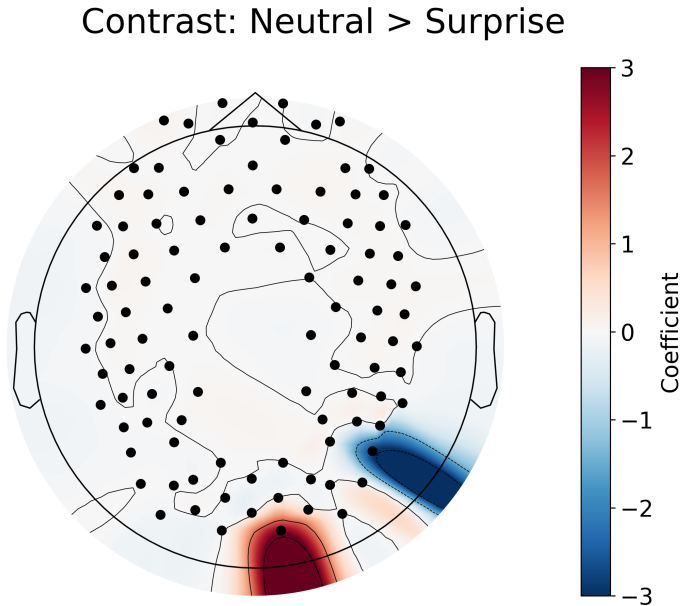


Figure 3.4: GLM results for the contrast between neutral and surprise condition.

### 3.1.3 Face Type $\times$ Emotion differences in occipital regions

The interaction of Real  $>$  Virt within each emotion, as shown in Figure 3.5 revealed significant differences in occipital regions exclusively. For disgust, real faces elicited greater activation in the right occipital region compared to virtual faces, while the left occipital region showed the opposite pattern. For Joy and Neutral emotions, real faces also elicited greater activation in the occipital regions compared to virtual faces. For Sadness, the left occipital region showed greater activation for virtual faces compared to real faces. These findings suggest that the neural response to emotional expressions is modulated by the realism of the face stimuli.

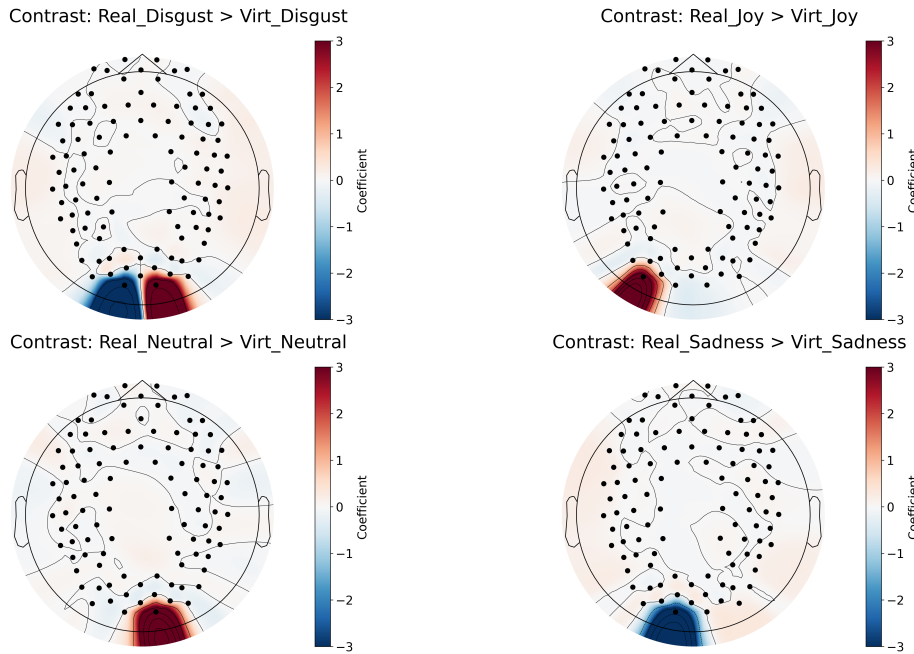


Figure 3.5: GLM results for the contrast between real and virtual conditions within each emotion.

The full table of the GLM contrasts for all main effects and interactions can be found in Appendix A.

## 3.2 Functional Connectivity

### 3.2.1 Face Type differentiated by greater connectivity for real faces

A main effect of Face type revealed significant differences in connectivity across ROI's. Most ROI's showed higher connectivity for real faces compared to virtual faces, with a few exceptions, i.e. the left occipital/parietal ROI, which showed higher connectivity for virtual faces compared to real faces. A mean  $t$ -value of 1.55 indicated the connectivity is generally higher for real faces compared to virtual faces across all ROI's.

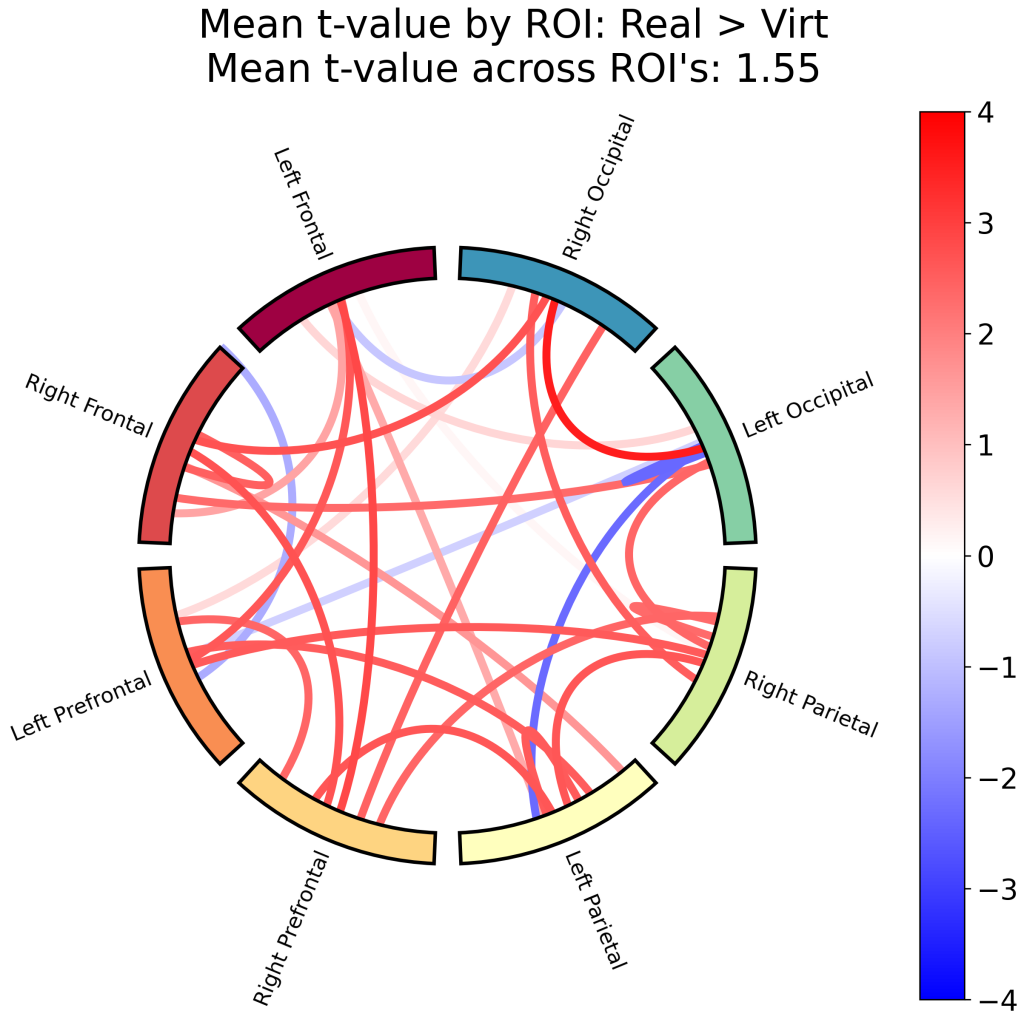


Figure 3.6: Functional connectivity results for the contrast between real and virtual conditions. Red signifies that condition 1 (real faces) has higher connectivity between those two ROI's than condition 2 (virtual faces), while blue signifies that condition 2 (virtual faces) has higher connectivity than condition 1 (real faces). The color bar on the right shows the  $t$ -statistic of the contrast, which indicates the strength of the difference in connectivity between the two conditions. The Mean  $t$ -value across ROI's is the average of the  $t$ -values for all significant channel pairs across all ROI's, and generally indicates whether the connectivity is higher or lower in one condition compared to the other. If this value is positive, it indicates that the connectivity is higher in condition 1 (real faces) than condition 2 (virtual faces), and vice versa.

### 3.2.2 Emotion differentiated by higher connectivity for Anger and Fear

The emotion contrasts (as shown in Figure 3.7) revealed significant differences in functional connectivity across different emotions and ROI's. The  $t$ -values show that Anger and Fear showed higher connectivity in general compared to the other emotions, and when compared to each other, Fear has only slightly higher connectivity than Anger. This higher connectivity for Anger and Fear as compared to the other emotions is consistent across most ROI's as well. The rest of the emotion contrasts can be found in Appendix B, which shows the remaining set of contrasts for all emotions.

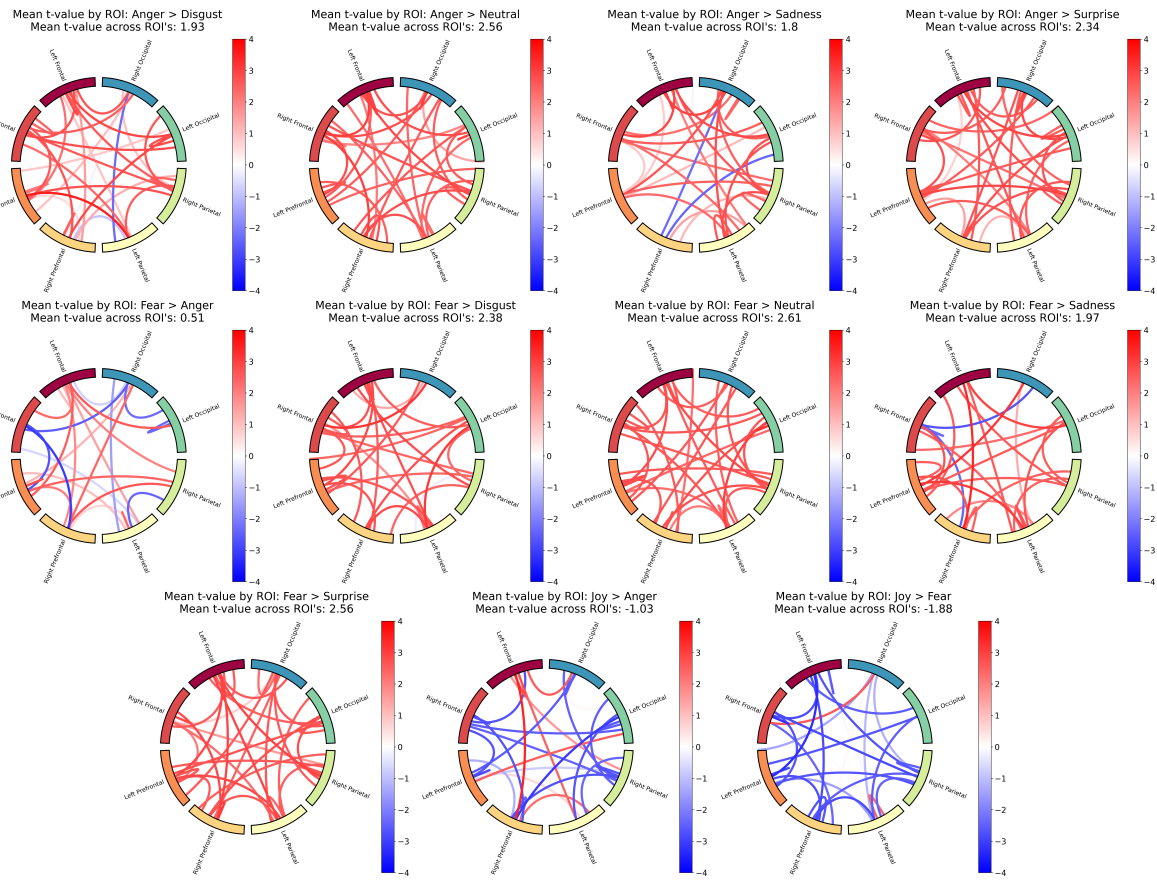


Figure 3.7: Functional connectivity results for Fear and Anger vs. the other emotions.

This summary of the functional connectivity results for the contrasts between different emotions (as shown in Figure 3.8) shows that Anger and Fear have the highest

connectivity compared to the other emotions, with Fear having slightly higher connectivity than Anger. This lines up with Figure 3.7, which shows that Anger and Fear have higher connectivity compared to the other emotions.

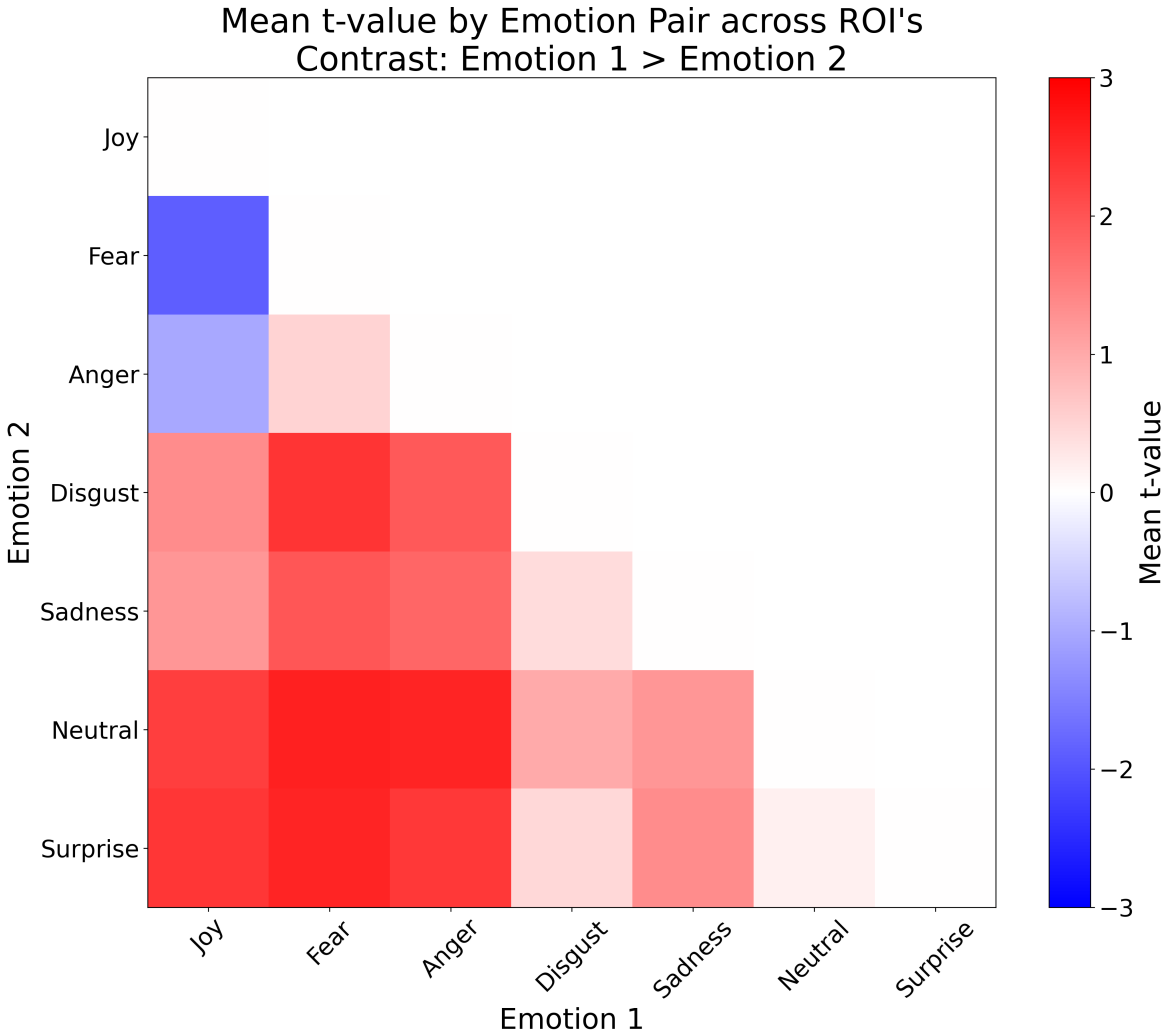


Figure 3.8: A heatmap summary of the functional connectivity results for the contrasts between different emotions. Red signifies that emotion 1 has higher connectivity than emotion 2, while blue signifies that emotion 2 has higher connectivity than emotion 1. The color bar on the right shows the  $t$ -value averaged across all significant channel pairs and across all ROI's, which indicates the strength of the difference in connectivity between the two emotions. This is the same value that is shown at the top of each plot in Figure 3.6 and Figure 3.7.

The count of significantly different channel pairs for each ROI summed across all emotions (as shown in Figure 3.9) marks 3 regions with an asterisk, these regions have less

channel pairs that are significantly different from each other, meaning that these regions are more synchronized with each other than any other pair of ROI's. These regions are the left occipital/right occipital, left occipital/left occipital, and right occipital/right occipital ROI's. This indicates that the differences in processing emotions occur in the frontal, prefrontal, and parietal regions of the brain.

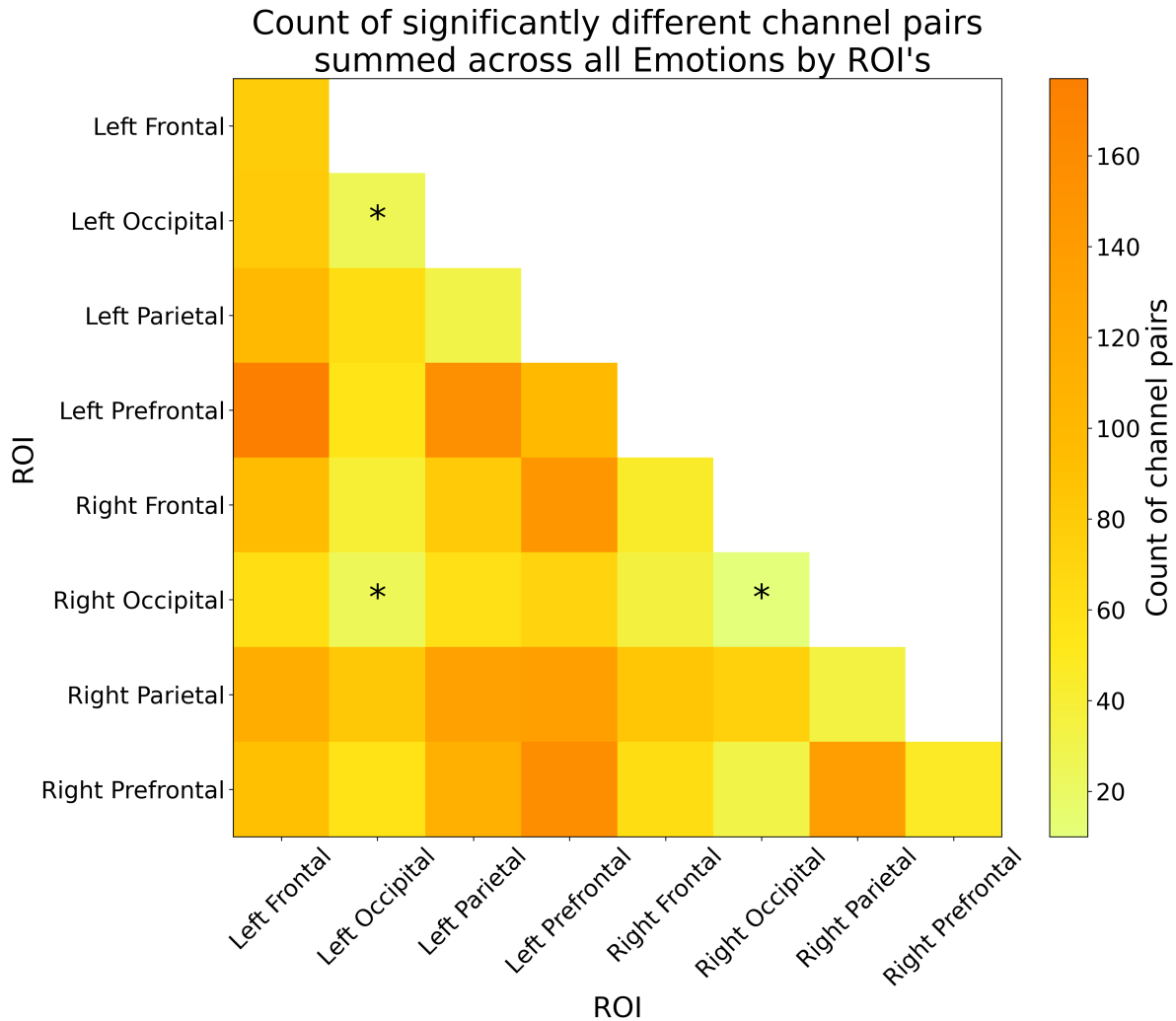


Figure 3.9: A heatmap summary of the number of significantly different channel pairs for each ROI summed across all emotions. The color bar on the right shows the number of significant channel pairs for each ROI, with brighter colors indicating a smaller number of significant channel pairs, and darker colors indicating a larger number of significant channel pairs. An asterisk was placed on the 3 ROI's with the least number of significantly different channel pairs to indicate that these ROI's are more synchronized with each other than any other pair of ROI's, regardless of the emotion. Note that ROI's can have differences within them, as each ROI is made up of multiple channels, and the differences are calculated between channels within the same ROI.

### 3.2.3 Face Type $\times$ Emotion differentiated by higher connectivity for real faces in Anger, Disgust, and Neutral

The interaction of face type with emotion (Real > Virt within each emotion as shown in Figure 3.10) revealed significant differences in functional connectivity across both face types within each emotion. For Anger, Disgust, Fear, and Neutral, virtual faces showed higher connectivity across most ROI's compared to real faces, whereas for Joy, Sadness, and Surprise, real faces showed higher connectivity across most ROI's compared to virtual faces. Like the GLM results, this indicates that the neural response to emotional expressions is modulated by the realism of the face stimuli, with different patterns of connectivity observed for each face type  $\times$  emotion interaction.

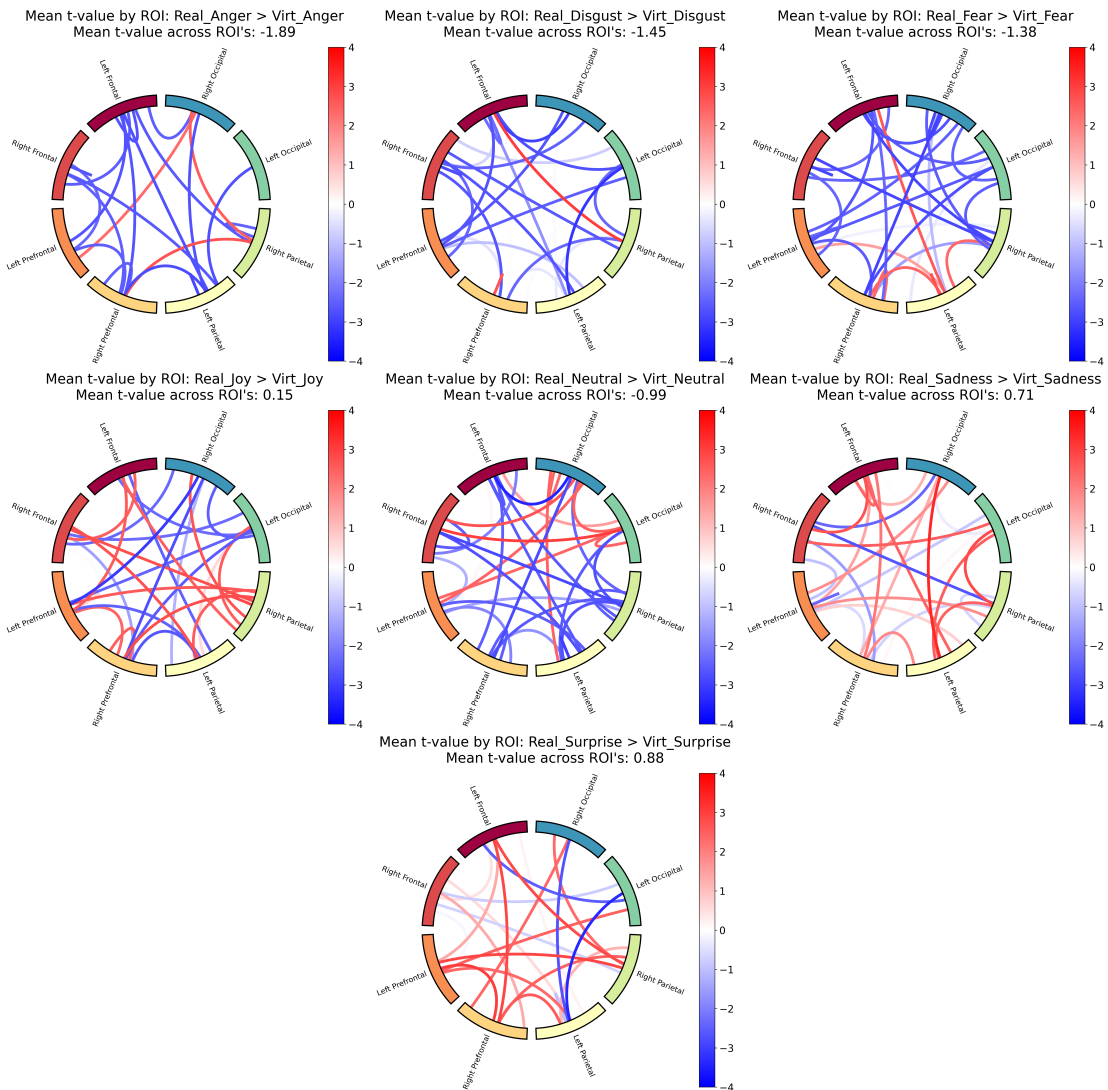


Figure 3.10: Functional connectivity results for the contrast between real and virtual conditions within each emotion.

The full table of the functional connectivity contrasts for all main effects and interactions can be found in Appendix B.

### 3.3 Higher accuracy for real faces in the memory task

A two-way Type III ANOVA revealed a significant main effect of face type,  $F(1, 4802) = 7.96, p = 0.0048$ , indicating that memory performance was higher for real faces compared to virtual faces, as shown in Figure 3.11. There was no significant main effect of emotion,  $F(6, 4802) = 0.83, p = 0.55$ , nor a significant interaction between face type and emotion,  $F(6, 4802) = 0.46, p = 0.84$ . These findings suggest that while the realism of the face influences memory performance, the specific emotional expression does not have a significant impact on memory accuracy.

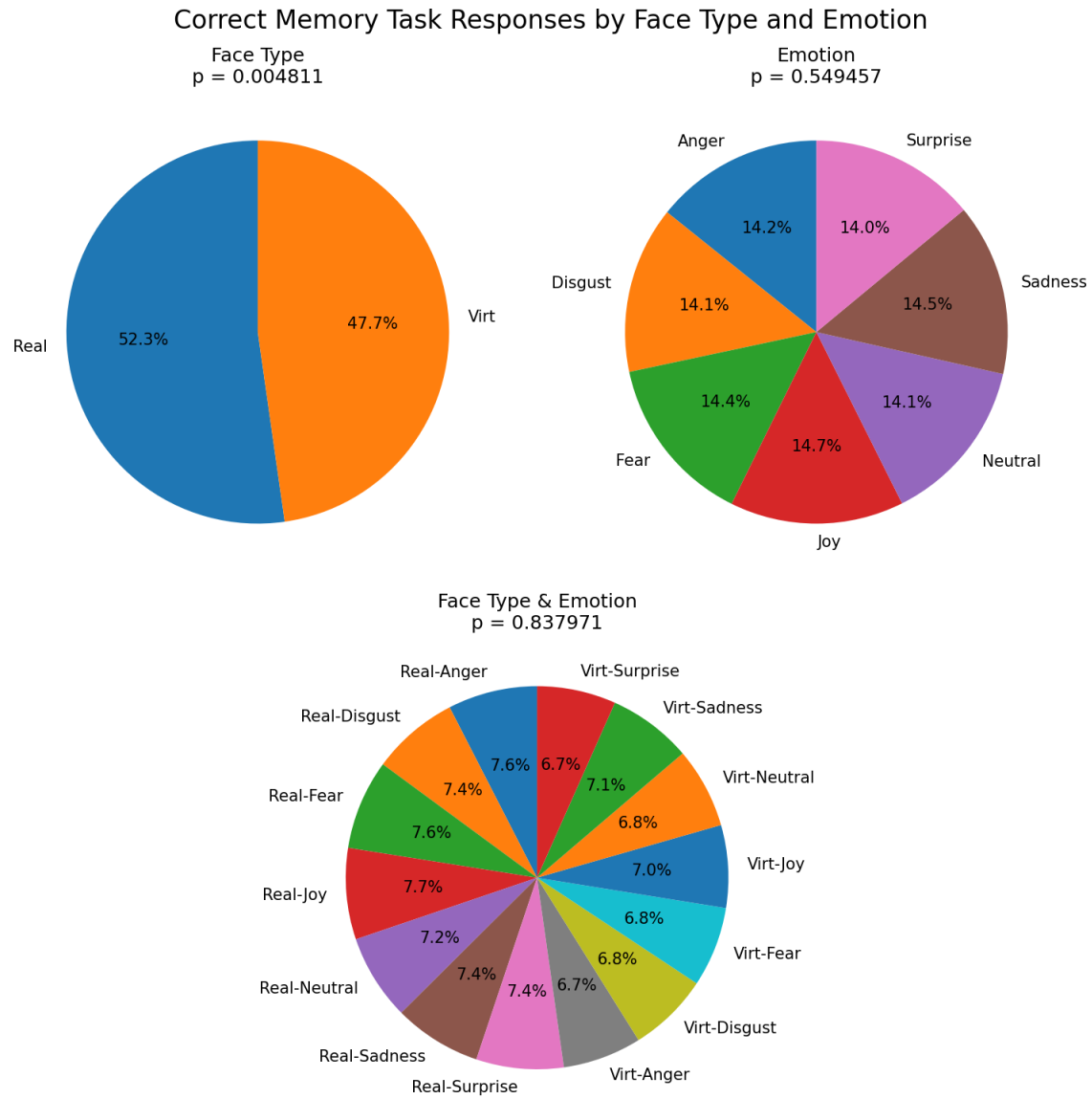


Figure 3.11: Proportion correct by condition in the memory task, plotted separately for real and virtual faces, for each emotion, and the interaction between face type and emotion. The  $p$ -values indicate the significance of the main effects and interaction.

The full ANOVA table is shown in Appendix C.1.

# **Chapter 4**

## **Discussion**

### **4.1 Limitations and Future Directions**

### **4.2 Conclusion**

# Bibliography

- Bastos, A. M. and Schoffelen, J.-M. (2016). A Tutorial Review of Functional Connectivity Analysis Methods and Their Interpretational Pitfalls. *Frontiers in Systems Neuroscience*, 9. Publisher: Frontiers.
- Bergmann, T., Froese, L., Gomez, A., Sainbhi, A. S., Vakitbilir, N., Islam, A., Stein, K., Marquez, I., Amenta, F., Park, K., Ibrahim, Y., and Zeiler, F. A. (2023). Evaluation of Morlet Wavelet Analysis for Artifact Detection in Low-Frequency Commercial Near-Infrared Spectroscopy Systems. *Bioengineering*, 11(1):0.
- Bulgarelli, C., Blasi, A., McCann, S., Milosavljevic, B., Ghillia, G., Mbye, E., Touray, E., Fadera, T., Acolatse, L., Moore, S. E., Lloyd-Fox, S., Elwell, C. E., Eggebrecht, A. T., and Team, t. B. S. (2025). Growth in early infancy drives optimal brain functional connectivity which predicts cognitive flexibility in later childhood. Pages: 2024.01.02.573930 Section: New Results.
- Conley, M. I., Dellarco, D. V., Rubien-Thomas, E., Cohen, A. O., Cervera, A., Tottenham, N., and Casey, B. (2018). The racially diverse affective expression (RADIATE) face stimulus set. *Psychiatry Research*, 270:1059–1067.
- Cui, X., Bray, S., and Reiss, A. L. (2010). Functional near infrared spectroscopy (NIRS) signal improvement based on negative correlation between oxygenated and deoxygenated hemoglobin dynamics. *NeuroImage*, 49(4):3039–3046.

- Ekman, P. (1992). Are there basic emotions? *Psychological Review*, 99(3):550–553. Place: US Publisher: American Psychological Association.
- Fishburn, F. A., Ludlum, R. S., Vaidya, C. J., and Medvedev, A. V. (2019). Temporal Derivative Distribution Repair (TDDR): A motion correction method for fNIRS. *NeuroImage*, 184:171–179.
- Friston, K. J. (2007). *Statistical parametric mapping: the analysis of functional brain images*. Elsevier / Academic Press, Amsterdam Boston, 1st ed edition.
- Gramfort, A., Luessi, M., Larson, E., Engemann, D. A., Strohmeier, D., Brodbeck, C., Goj, R., Jas, M., Brooks, T., Parkkonen, L., and Hämäläinen, M. (2013). MEG and EEG data analysis with MNE-Python. *Frontiers in Neuroscience*, 7. Publisher: Frontiers.
- Hakim, U., De Felice, S., Pinti, P., Zhang, X., Noah, J., Ono, Y., Burgess, P. W., Hamilton, A., Hirsch, J., and Tachtsidis, I. (2023). Quantification of inter-brain coupling: A review of current methods used in haemodynamic and electrophysiological hyperscanning studies. *NeuroImage*, 280:120354.
- Hernandez, S. M. and Pollonini, L. (2020). NIRSpot: A Tool for Quality Assessment of fNIRS Scans. In *Biophotonics Congress: Biomedical Optics 2020 (Translational, Microscopy, OCT, OTS, BRAIN)*, page BM2C.5, Washington, DC. Optica Publishing Group.
- Hocke, L. M., Oni, I. K., Duszynski, C. C., Corrigan, A. V., Frederick, B. D., and Dunn, J. F. (2018). Automated Processing of fNIRS Data—A Visual Guide to the Pitfalls and Consequences. *Algorithms*, 11(5):67. Number: 5 Publisher: Multidisciplinary Digital Publishing Institute.
- Holmes, M., Aalto, D., and Cummine, J. (2024). Opening the dialogue: A preliminary

- exploration of hair color, hair cleanliness, light, and motion effects on fNIRS signal quality. *PLOS ONE*, 19(5):e0304356. Publisher: Public Library of Science.
- Hu, P., Wang, P., Zhao, R., Yang, H., and Biswal, B. B. (2023). Characterizing the spatiotemporal features of functional connectivity across the white matter and gray matter during the naturalistic condition. *Frontiers in Neuroscience*, 17. Publisher: Frontiers.
- Kinder, K. T., Heim, H. L. R., Parker, J., Lowery, K., McCraw, A., Eddings, R. N., Defenderfer, J., Sullivan, J., and Buss, A. T. (2022). Systematic review of fNIRS studies reveals inconsistent chromophore data reporting practices. *Neurophotonics*, 9(4):040601.
- Kocsis, L., Herman, P., and Eke, A. (2006). The modified Beer–Lambert law revisited. *Physics in Medicine & Biology*, 51(5):N91.
- Lindquist, K. A., Wager, T. D., Kober, H., Bliss-Moreau, E., and Barrett, L. F. (2012). The brain basis of emotion: A meta-analytic review. *Behavioral and Brain Sciences*, 35(3):121–143.
- Luke, R., Larson, E. D., Shader, M. J., Innes-Brown, H., Yper, L. V., Lee, A. K. C., Sowman, P. F., and McAlpine, D. (2021). Analysis methods for measuring passive auditory fNIRS responses generated by a block-design paradigm. *Neurophotonics*, 8(2):025008. Publisher: SPIE.
- Miranda de Sá, A. M. F. L., Ferreira, D. D., Dias, E. W., Mendes, E. M. A. M., and Felix, L. B. (2009). Coherence estimate between a random and a periodic signal: Bias, variance, analytical critical values, and normalizing transforms. *Journal of the Franklin Institute*, 346(9):841–853.
- Oliver, M. M. and Amengual Alcover, E. (2020). UIBVFED: Virtual facial expression dataset. *PLOS ONE*, 15(4):e0231266.

- Peirce, J., Gray, J. R., Simpson, S., MacAskill, M., Höchenberger, R., Sogo, H., Kastman, E., and Lindeløv, J. K. (2019). PsychoPy2: Experiments in behavior made easy. *Behavior Research Methods*, 51(1):195–203.
- Pinti, P., Scholkmann, F., Hamilton, A., Burgess, P., and Tachtsidis, I. (2019). Current Status and Issues Regarding Pre-processing of fNIRS Neuroimaging Data: An Investigation of Diverse Signal Filtering Methods Within a General Linear Model Framework. *Frontiers in Human Neuroscience*, 12.
- Pollonini, L., Bortfeld, H., and Oghalai, J. S. (2016). PHOEBE: a method for real time mapping of optodes-scalp coupling in functional near-infrared spectroscopy. *Biomedical Optics Express*, 7(12):5104–5119. Publisher: Optica Publishing Group.
- Reddy, P., Izzetoglu, M., Shewokis, P. A., Sangobowale, M., Diaz-Arrastia, R., and Izzetoglu, K. (2021). Evaluation of fNIRS signal components elicited by cognitive and hypercapnic stimuli. *Scientific Reports*, 11(1):23457. Publisher: Nature Publishing Group.
- Scholkmann, F., Metz, A. J., and Wolf, M. (2014). Measuring tissue hemodynamics and oxygenation by continuous-wave functional near-infrared spectroscopy—how robust are the different calculation methods against movement artifacts? *Physiological Measurement*, 35(4):717. Publisher: IOP Publishing.
- Seabold, S. and Perktold, J. (2010). statsmodels: Econometric and statistical modeling with python. In *9th Python in Science Conference*.
- Singh, A. K. and Dan, I. (2006). Exploring the false discovery rate in multichannel NIRS. *NeuroImage*, 33(2):542–549.
- Tachtsidis, I. and Scholkmann, F. (2016). False positives and false negatives in functional near-infrared spectroscopy: issues, challenges, and the way forward. *Neurophotonics*, 3(3):031405. Publisher: SPIE.

Xu, G., Zhang, M., Wang, Y., Liu, Z., Huo, C., Li, Z., and Huo, M. (2017). Functional connectivity analysis of distracted drivers based on the wavelet phase coherence of functional near-infrared spectroscopy signals. *PLOS ONE*, 12(11):e0188329. Publisher: Public Library of Science.

# Appendix A

## GLM Contrasts

Table A.1: Table of contrast results from the GLM analysis.

Contrast	Region	Ch Name	Coef.	Std.Err.	<i>z</i>	<i>p<sub>fdr</sub></i>
Real > Virt	Left Occipital	S23 D15 hbt	-1.550	0.394	-3.937	0.009
Joy > Neutral	Right Parietal	S20 D29 hbt	2.611	0.623	4.194	0.001
Joy > Neutral	Right Occipital	S23 D30 hbt	-3.144	0.623	-5.050	0.000
Joy > Surprise	Right Occipital	S23 D16 hbt	-2.884	0.647	-4.460	0.001
Joy > Surprise	Left Prefrontal	S25 D6 hbt	-2.379	0.647	-3.679	0.012
Fear > Neutral	Right Occipital	S23 D30 hbt	-2.126	0.557	-3.819	0.014
Fear > Surprise	Right Parietal	S20 D29 hbt	-2.048	0.568	-3.606	0.032
Anger > Neutral	Right Occipital	S23 D30 hbt	-3.620	0.652	-5.547	0.000
Disgust > Surprise	Right Occipital	S23 D16 hbt	-2.507	0.640	-3.920	0.005
Disgust > Surprise	Left Prefrontal	S25 D6 hbt	-2.531	0.640	-3.958	0.005
Sadness > Neutral	Left Frontal	S4 D6 hbt	-2.257	0.601	-3.754	0.018
Sadness > Surprise	Left Frontal	S4 D6 hbt	-2.610	0.673	-3.879	0.011
Sadness > Surprise	Right Parietal	S20 D29 hbt	-2.304	0.673	-3.425	0.032

Continued on next page

Table A.1: Table of contrast results from the GLM analysis.

Contrast	Region	Ch Name	Coef.	Std.Err.	<i>z</i>	<i>p</i> <sub>fdr</sub>
Neutral > Surprise	Right Parietal	S20 D29 hbt	-2.653	0.625	-4.247	0.002
Neutral > Surprise	Right Occipital	S23 D30 hbt	2.461	0.625	3.940	0.004
Real Joy > Real Disgust	Right Occipital	S23 D30 hbt	-5.344	1.093	-4.889	0.000
Real Joy > Real Sadness	Right Occipital	S24 D30 hbt	-3.816	0.964	-3.958	0.008
Real Joy > Real Neutral	Right Occipital	S23 D30 hbt	-5.786	0.980	-5.906	0.000
Real Joy > Real Surprise	Right Frontal	S9 D19 hbt	3.093	0.997	3.101	0.050
Real Joy > Real Surprise	Left Occipital	S23 D15 hbt	-3.754	0.997	-3.764	0.017
Real Joy > Real Surprise	Right Occipital	S23 D16 hbt	-3.577	0.997	-3.587	0.017
Real Joy > Real Surprise	Left Prefrontal	S25 D6 hbt	-3.293	0.997	-3.302	0.033
Real Joy > Virt Joy	Left Occipital	S32 D15 hbt	3.484	0.966	3.607	0.032
Real Joy > Virt Fear	Left Occipital	S23 D15 hbt	-3.384	0.965	-3.506	0.023
Real Joy > Virt Fear	Right Occipital	S23 D30 hbt	-3.649	0.965	-3.781	0.016
Real Joy > Virt Disgust	Left Occipital	S23 D15 hbt	-4.428	0.986	-4.490	0.001
Real Joy > Virt Sadness	Left Occipital	S23 D15 hbt	-4.435	0.973	-4.556	0.001
Real Joy > Virt Surprise	Right Occipital	S23 D16 hbt	-3.197	0.949	-3.368	0.039
Real Joy > Virt Surprise	Right Occipital	S23 D30 hbt	-3.410	0.949	-3.593	0.034
Real Fear > Real Disgust	Right Occipital	S23 D30 hbt	-4.918	1.087	-4.522	0.001
Real Fear > Real Neutral	Right Occipital	S23 D30 hbt	-5.360	0.980	-5.470	0.000
Real Fear > Virt Joy	Left Prefrontal	S25 D6 hbt	4.150	1.054	3.938	0.008
Real Fear > Virt Disgust	Left Occipital	S23 D15 hbt	-4.112	1.009	-4.073	0.002
Real Fear > Virt Disgust	Left Prefrontal	S25 D6 hbt	4.183	1.009	4.144	0.002
Real Fear > Virt Sadness	Left Occipital	S23 D15 hbt	-4.119	1.003	-4.109	0.004
Real Fear > Virt Sadness	Left Prefrontal	S25 D6 hbt	3.595	1.003	3.585	0.017

Continued on next page

Table A.1: Table of contrast results from the GLM analysis.

Contrast	Region	Ch Name	Coef.	Std.Err.	<i>z</i>	<i>p</i> <sub>fdr</sub>
Real Anger > Real Disgust	Right Occipital	S23 D30 hbt	-4.697	1.117	-4.205	0.003
Real Anger > Real Neutral	Right Occipital	S23 D30 hbt	-5.139	0.983	-5.226	0.000
Real Disgust > Real Surprise	Left Frontal	S4 D6 hbt	-3.742	1.107	-3.380	0.025
Real Disgust > Real Surprise	Left Occipital	S23 D15 hbt	-4.679	1.107	-4.226	0.002
Real Disgust > Real Surprise	Right Occipital	S23 D30 hbt	4.221	1.107	3.813	0.007
Real Disgust > Virt Fear	Left Occipital	S23 D15 hbt	-4.309	1.013	-4.252	0.002
Real Disgust > Virt Disgust	Left Occipital	S23 D15 hbt	-5.353	1.163	-4.603	0.000
Real Disgust > Virt Disgust	Right Occipital	S23 D30 hbt	5.028	1.163	4.323	0.001
Real Disgust > Virt Sadness	Left Occipital	S23 D15 hbt	-5.360	1.163	-4.608	0.000
Real Disgust > Virt Sadness	Right Occipital	S23 D30 hbt	4.254	1.163	3.657	0.013
Real Disgust > Virt Neutral	Right Occipital	S23 D30 hbt	3.878	1.102	3.520	0.044
Real Sadness > Real Neutral	Right Occipital	S23 D30 hbt	-3.749	0.912	-4.110	0.002
Real Sadness > Real Neutral	Right Occipital	S24 D30 hbt	4.012	0.912	4.398	0.001
Real Sadness > Real Surprise	Left Frontal	S4 D6 hbt	-3.743	1.059	-3.534	0.021
Real Sadness > Real Surprise	Right Occipital	S24 D30 hbt	4.688	1.059	4.426	0.001
Real Sadness > Virt Joy	Right Occipital	S24 D30 hbt	3.811	1.048	3.638	0.028
Real Sadness > Virt Disgust	Left Occipital	S23 D15 hbt	-3.951	1.088	-3.633	0.029
Real Sadness > Virt Sadness	Left Occipital	S23 D15 hbt	-3.959	1.051	-3.766	0.017
Real Neutral > Real Surprise	Right Parietal	S20 D29 hbt	-3.553	0.933	-3.809	0.007
Real Neutral > Real Surprise	Right Occipital	S23 D30 hbt	4.663	0.933	4.999	0.000
Real Neutral > Virt Joy	Right Occipital	S23 D30 hbt	3.563	0.924	3.856	0.012
Real Neutral > Virt Anger	Left Frontal	S4 D6 hbt	4.371	1.009	4.330	0.002
Real Neutral > Virt Anger	Right Occipital	S23 D30 hbt	3.737	1.009	3.702	0.011

Continued on next page

Table A.1: Table of contrast results from the GLM analysis.

Contrast	Region	Ch Name	Coef.	Std.Err.	<i>z</i>	<i>p</i> <sub>fdr</sub>
Real Neutral > Virt Disgust	Right Occipital	S23 D30 hbt	5.470	1.020	5.365	0.000
Real Neutral > Virt Sadness	Left Frontal	S4 D6 hbt	4.863	0.963	5.051	0.000
Real Neutral > Virt Sadness	Right Occipital	S23 D30 hbt	4.696	0.963	4.877	0.000
Real Neutral > Virt Neutral	Right Occipital	S23 D30 hbt	4.320	0.994	4.346	0.001
Real Surprise > Virt Joy	Left Frontal	S4 D6 hbt	3.580	1.038	3.448	0.029
Real Surprise > Virt Joy	Left Prefrontal	S25 D6 hbt	4.185	1.038	4.030	0.006
Real Surprise > Virt Anger	Left Frontal	S4 D6 hbt	5.443	1.096	4.966	0.000
Real Surprise > Virt Anger	Right Frontal	S10 D17 hbt	-3.659	1.096	-3.338	0.029
Real Surprise > Virt Anger	Left Occipital	S23 D15 hbt	3.907	1.096	3.565	0.019
Real Surprise > Virt Disgust	Left Prefrontal	S25 D6 hbt	4.218	1.042	4.048	0.005
Real Surprise > Virt Sadness	Left Frontal	S4 D6 hbt	5.935	1.000	5.937	0.000
Real Surprise > Virt Sadness	Left Prefrontal	S7 D6 hbt	3.660	1.000	3.661	0.007
Real Surprise > Virt Sadness	Right Parietal	S20 D29 hbt	4.101	1.000	4.102	0.002
Real Surprise > Virt Sadness	Left Prefrontal	S25 D6 hbt	3.630	1.000	3.631	0.007
Real Surprise > Virt Neutral	Left Frontal	S4 D6 hbt	3.189	1.025	3.111	0.048
Real Surprise > Virt Neutral	Right Frontal	S9 D19 hbt	-3.357	1.025	-3.275	0.048
Real Surprise > Virt Neutral	Right Parietal	S20 D29 hbt	3.539	1.025	3.453	0.048
Real Surprise > Virt Neutral	Left Occipital	S31 D15 hbt	-3.254	1.025	-3.174	0.048
Virt Joy > Virt Disgust	Left Occipital	S32 D15 hbt	-4.343	1.008	-4.308	0.002
Virt Fear > Virt Disgust	Right Occipital	S23 D30 hbt	3.333	0.928	3.590	0.034
Virt Fear > Virt Sadness	Left Frontal	S4 D6 hbt	3.597	1.021	3.522	0.044
Virt Anger > Virt Disgust	Left Frontal	S4 D6 hbt	-3.633	1.033	-3.518	0.019
Virt Anger > Virt Disgust	Left Occipital	S23 D15 hbt	-4.581	1.033	-4.436	0.001

Continued on next page

Table A.1: Table of contrast results from the GLM analysis.

Contrast	Region	Ch Name	Coef.	Std.Err.	<i>z</i>	<i>p<sub>fdr</sub></i>
Virt Anger > Virt Disgust	Left Prefrontal	S25 D6 hbt	3.565	1.033	3.452	0.019
Virt Anger > Virt Sadness	Left Occipital	S23 D15 hbt	-4.589	1.018	-4.508	0.001
Virt Disgust > Virt Sadness	Left Frontal	S4 D6 hbt	4.125	1.044	3.950	0.008
Virt Disgust > Virt Surprise	Left Occipital	S23 D15 hbt	3.761	1.001	3.758	0.018
Virt Sadness > Virt Surprise	Left Occipital	S23 D15 hbt	3.768	0.978	3.853	0.012

# Appendix B

## Functional Connectivity Contrasts

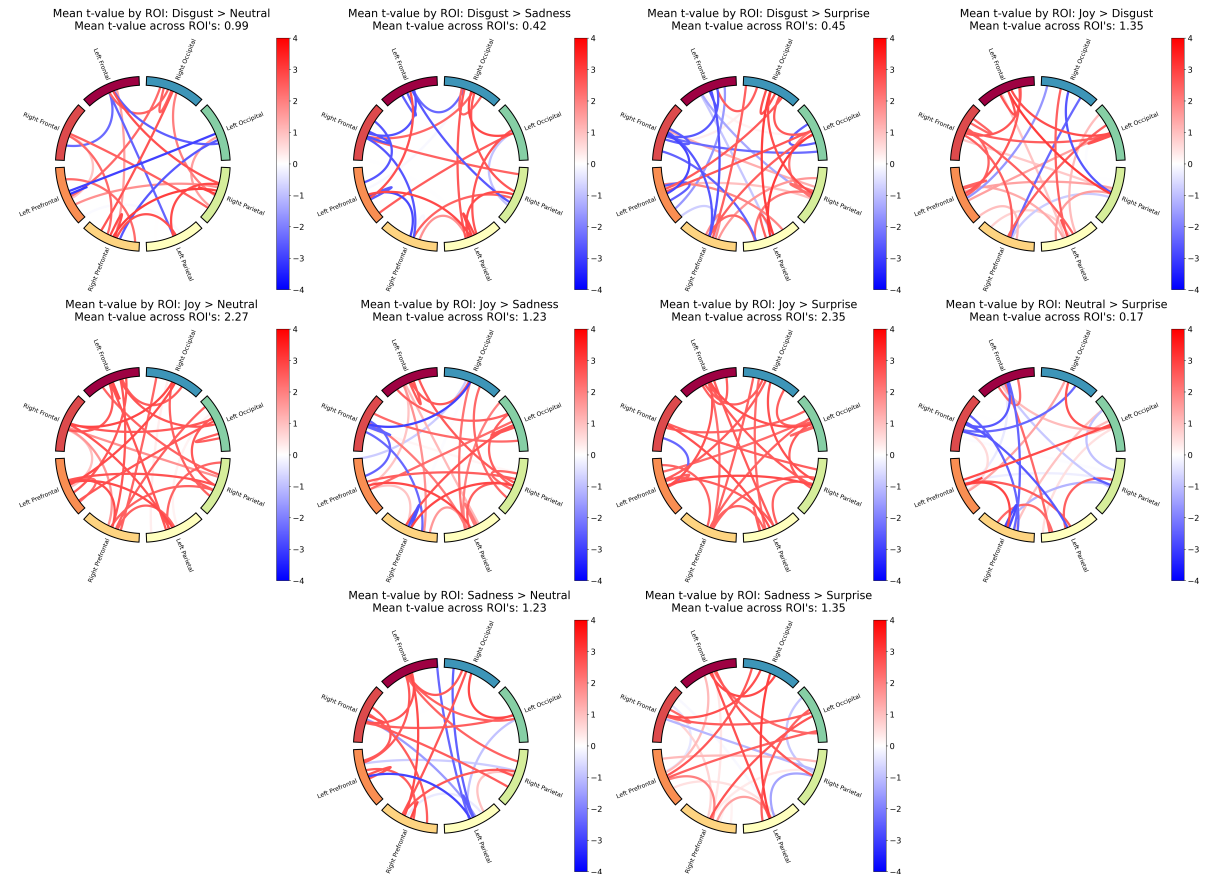


Figure B.1: Functional connectivity results for the rest of the contrasts. Same concept as explained in figure 3.6. These are the rest of the contrasts that were not shown in 3.7.

Table B.1: Group level  $t$ -tests and Sum of Significantly different channels averaged across ROIs.

Contrast	Mean $t$ value	Sum of Sig. diff channels
Real > Virt	1.546	114.000
Joy > Fear	-1.880	118.000
Joy > Anger	-1.025	65.000
Joy > Disgust	1.354	135.000
Joy > Sadness	1.229	127.000
Joy > Neutral	2.269	113.000
Joy > Surprise	2.346	84.000
Fear > Anger	0.511	113.000
Fear > Disgust	2.382	196.000
Fear > Sadness	1.975	89.000
Fear > Neutral	2.615	263.000
Fear > Surprise	2.558	290.000
Anger > Disgust	1.929	164.000
Anger > Sadness	1.797	158.000
Anger > Neutral	2.565	185.000
Anger > Surprise	2.335	194.000
Disgust > Sadness	0.415	71.000
Disgust > Neutral	0.994	93.000
Disgust > Surprise	0.447	128.000
Sadness > Neutral	1.232	90.000
Sadness > Surprise	1.352	100.000
Neutral > Surprise	0.172	104.000

Continued on next page

Table B.1: Group level  $t$ -tests and Sum of Significantly different channels averaged across ROIs.

Contrast	Mean $t$ value	Sum of Sig. diff channels
Real Joy > Real Fear	-0.243	109.000
Real Joy > Real Anger	-1.058	97.000
Real Joy > Real Disgust	2.089	84.000
Real Joy > Real Sadness	-0.986	154.000
Real Joy > Real Neutral	1.012	201.000
Real Joy > Real Surprise	0.676	124.000
Real Joy > Virt Joy	0.148	130.000
Real Joy > Virt Fear	-2.114	136.000
Real Joy > Virt Anger	-2.618	132.000
Real Joy > Virt Disgust	-1.637	99.000
Real Joy > Virt Sadness	0.285	93.000
Real Joy > Virt Neutral	0.204	76.000
Real Joy > Virt Surprise	1.456	117.000
Real Fear > Real Anger	-0.969	126.000
Real Fear > Real Disgust	1.906	119.000
Real Fear > Real Sadness	0.270	61.000
Real Fear > Real Neutral	1.413	167.000
Real Fear > Real Surprise	0.687	110.000
Real Fear > Virt Joy	0.371	129.000
Real Fear > Virt Fear	-1.376	90.000
Real Fear > Virt Anger	-2.352	167.000
Real Fear > Virt Disgust	0.075	78.000

Continued on next page

Table B.1: Group level  $t$ -tests and Sum of Significantly different channels averaged across ROIs.

Contrast	Mean $t$ value	Sum of Sig. diff channels
Real Fear > Virt Sadness	1.073	118.000
Real Fear > Virt Neutral	0.983	101.000
Real Fear > Virt Surprise	1.805	136.000
Real Anger > Real Disgust	2.054	158.000
Real Anger > Real Sadness	0.545	113.000
Real Anger > Real Neutral	1.915	191.000
Real Anger > Real Surprise	1.773	115.000
Real Anger > Virt Joy	1.931	141.000
Real Anger > Virt Fear	-0.996	85.000
Real Anger > Virt Anger	-1.887	70.000
Real Anger > Virt Disgust	0.840	103.000
Real Anger > Virt Sadness	1.050	134.000
Real Anger > Virt Neutral	1.744	109.000
Real Anger > Virt Surprise	1.377	217.000
Real Disgust > Real Sadness	-1.856	106.000
Real Disgust > Real Neutral	0.347	124.000
Real Disgust > Real Surprise	-0.980	130.000
Real Disgust > Virt Joy	-0.600	96.000
Real Disgust > Virt Fear	-2.206	146.000
Real Disgust > Virt Anger	-2.606	284.000
Real Disgust > Virt Disgust	-1.452	66.000
Real Disgust > Virt Sadness	-0.670	121.000

Continued on next page

Table B.1: Group level  $t$ -tests and Sum of Significantly different channels averaged across ROIs.

Contrast	Mean $t$ value	Sum of Sig. diff channels
Real Disgust > Virt Neutral	-0.843	83.000
Real Disgust > Virt Surprise	-0.139	69.000
Real Sadness > Real Neutral	1.797	128.000
Real Sadness > Real Surprise	1.771	97.000
Real Sadness > Virt Joy	1.686	124.000
Real Sadness > Virt Fear	-0.656	33.000
Real Sadness > Virt Anger	-2.204	80.000
Real Sadness > Virt Disgust	-0.303	56.000
Real Sadness > Virt Sadness	0.713	107.000
Real Sadness > Virt Neutral	1.475	47.000
Real Sadness > Virt Surprise	2.301	104.000
Real Neutral > Real Surprise	-0.638	173.000
Real Neutral > Virt Joy	-1.072	67.000
Real Neutral > Virt Fear	-2.179	255.000
Real Neutral > Virt Anger	-2.525	322.000
Real Neutral > Virt Disgust	-2.123	139.000
Real Neutral > Virt Sadness	-0.900	151.000
Real Neutral > Virt Neutral	-0.988	102.000
Real Neutral > Virt Surprise	0.344	143.000
Real Surprise > Virt Joy	0.824	120.000
Real Surprise > Virt Fear	-2.407	136.000
Real Surprise > Virt Anger	-2.482	167.000

Continued on next page

Table B.1: Group level  $t$ -tests and Sum of Significantly different channels averaged across ROIs.

Contrast	Mean $t$ value	Sum of Sig. diff channels
Real Surprise > Virt Disgust	-1.044	80.000
Real Surprise > Virt Sadness	-0.182	73.000
Real Surprise > Virt Neutral	0.162	104.000
Real Surprise > Virt Surprise	0.883	88.000
Virt Joy > Virt Fear	-1.810	166.000
Virt Joy > Virt Anger	-2.421	189.000
Virt Joy > Virt Disgust	-1.524	129.000
Virt Joy > Virt Sadness	-0.185	118.000
Virt Joy > Virt Neutral	-0.695	103.000
Virt Joy > Virt Surprise	-0.287	80.000
Virt Fear > Virt Anger	-1.766	51.000
Virt Fear > Virt Disgust	1.338	72.000
Virt Fear > Virt Sadness	1.757	125.000
Virt Fear > Virt Neutral	2.267	114.000
Virt Fear > Virt Surprise	2.356	153.000
Virt Anger > Virt Disgust	2.054	138.000
Virt Anger > Virt Sadness	2.488	170.000
Virt Anger > Virt Neutral	2.373	128.000
Virt Anger > Virt Surprise	2.616	207.000
Virt Disgust > Virt Sadness	1.327	74.000
Virt Disgust > Virt Neutral	1.005	39.000
Virt Disgust > Virt Surprise	1.471	153.000

Continued on next page

Table B.1: Group level  $t$ -tests and Sum of Significantly different channels averaged across ROIs.

Contrast	Mean $t$ value	Sum of Sig. diff channels
Virt Sadness > Virt Neutral	-0.015	100.000
Virt Sadness > Virt Surprise	1.176	82.000
Virt Neutral > Virt Surprise	0.943	99.000

# Appendix C

## Memory Task

### C.1 ANOVA Results

Table C.1: Two-way ANOVA results for the effect of Face Type and Emotion and their interaction on the correct responses.

	sum_sq	df	F	PR(>F)
Intercept	261.07756	1.00000	1764.58989	0.00000
C(Face_Type)	1.17722	1.00000	7.95666	0.00481
C(Emotion)	0.73335	6.00000	0.82610	0.54946
C(Face_Type):C(Emotion)	0.40872	6.00000	0.46041	0.83797
Residual	710.47356	4802.00000		

## C.2 Memory Task No Response Distribution

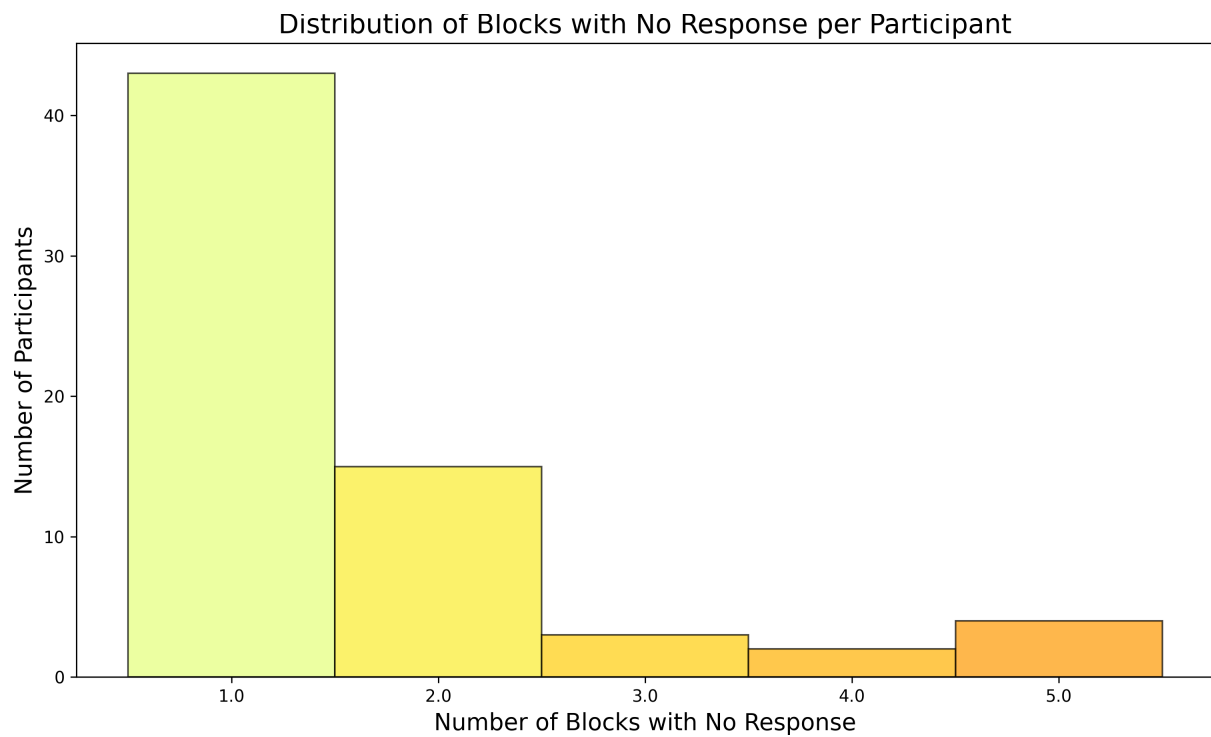


Figure C.1: Distribution of the number of no responses across the 56 blocks for each participant in the memory task.